Geosphere

The architecture of oceanic plateaus revealed by the volcanic stratigraphy of the accreted Wrangellia oceanic plateau

Andrew R. Greene, James S. Scoates, Dominique Weis, Erik C. Katvala, Steve Israel and Graham T. Nixon

Geosphere 2010;6;47-73
doi: 10.1130/GES00212.1

Notes

The architecture of oceanic plateaus revealed by the volcanic stratigraphy of the accreted Wrangellia oceanic plateau

Andrew R. Greene*
James S. Scoates
Dominique Weis
Pacific Centre for Isotopic and Geochemical Research, Department of Earth and Ocean Sciences, University of British Columbia, Vancouver, British Columbia V6T1Z4, Canada

Erik C. Katvala
Department of Geoscience, University of Calgary, 2500 University Drive NW, Calgary, Alberta T2N1N4, Canada

Steve Israel
Yukon Geological Survey, 2099-2nd Ave, Whitehorse, Yukon Y1A2C6, Canada

Graham T. Nixon
British Columbia Geological Survey, P.O. Box 9320, Station Provincial Government, Victoria, British Columbia V8W9N3, Canada

ABSTRACT

The accreted Wrangellia flood basalts and associated sedimentary rocks that compose the prevolcanic and postvolcanic stratigraphy provide an unparalleled view of the architecture, eruptive environment, and accumulation and subsidence history of an oceanic plateau. This Triassic large igneous province extends for ~2300 km in the Pacific Northwest of North America, from central Alaska and western Yukon (Nikolai Formation) to Vancouver Island (Karmutsen Formation), and contains exposures of submarine and subaerial volcanic rocks representing composite stratigraphic thicknesses of 3.5–6 km. Here we provide a model for the construction of the Wrangellia oceanic plateau using the following information and visualization tools: (1) stratigraphic summaries for different areas of Wrangellia; (2) new $^{40}Ar/^{39}Ar$ geochronology results; (3) compilation and assessment of geochronology and biostratigraphy for Wrangellia; (4) compiled digital geologic maps; (5) an online photographic archive of field relationships; and (6) a Google Earth file showing the mapped extent of Wrangellia flood basalts and linked field photographs.

Based on combined radiometric (U-Pb, $^{40}Ar/^{39}Ar$, K-Ar), paleontological, and magnetostratigraphic age constraints, the Wrangellia flood basalts were emplaced during a single phase of tholeiitic volcanism ca. 230–225 Ma, and possibly within as few as 2 Myr, onto preexisting submerged arc crust. There are distinct differences in volcanic stratigraphy and basement composition between Northern and Southern Wrangellia. On Vancouver Island, ~6 km of high-Ti basalts, with minor amounts of picrites, record an emergent sequence of pillow basalt, pillow breccia and hyaloclastite, and subaerial flows that overlie Devonian–Mississippian (ca. 380–355 Ma) island arc rocks and Mississippian–Permian marine sedimentary strata. In contrast, Alaska and Yukon contain 1–3.5-km-thick sequences of mostly subaerial high-Ti basalt flows, with low-Ti basalt and submarine pillow basalts in the lowest parts of the stratigraphy, that overlie Pennsylvanian–Permian (312–280 Ma) volcanic and sedimentary rocks. Subsidence of the entire plateau occurred during and after volcanism, based on late-stage interflow sedimentary lenses in the upper stratigraphic levels and the presence of hundreds of meters to >1000 m of overlying marine sedimentary rocks, predominantly limestone. The main factors that controlled the resulting volcanic architecture of the Wrangellia oceanic plateau include high effusion rates and the formation of extensive compound flow fields from low-viscosity, high-temperature tholeiitic basalts, sill-dominated feeder systems, limited repose time between flows (absence of weathering, erosion, sedimentation), submarine versus subaerial emplacement, and relative water depth (e.g., pillow basalt–volcaniclastic transition).

INTRODUCTION

Approximately 3% of the ocean floor is covered with oceanic plateaus or flood basalts, mostly in the western Pacific and Indian Oceans (Fig. 1; Coffin and Eldholm, 1994). These regions can rise thousand of meters above the ocean floor and rarely exhibit magnetic lineations like the surrounding seafloor (Ben-Avraham et al., 1981). Oceanic plateaus are produced from high volumetric output rates of magma generated by high-degree melting events that are distinct from melting beneath mid-ocean ridges. Most of what we know about the architecture of oceanic plateaus is based on obducted portions of oceanic plateaus, drilling of the volcanic sequences of extant oceanic plateaus, and geophysical studies of oceanic plateaus. Study of oceanic plateaus improves our understanding of the relationship between large igneous provinces (LIPs) and large melting events, mass extinctions, and continental growth (e.g., Kerr, 2003; Wignall, 2001).

*Present address: Department of Geology and Geophysics, University of Hawai'i at Mānoa, 1680 East-West Road, Honolulu, Hawai'i 96822, USA; agreene@soest.hawaii.edu.

Geosphere; February 2010; v. 6; no. 1; p. 47–73; doi: 10.1130/GES00212.1; 9 figures; 6 tables; 11 supplemental files.

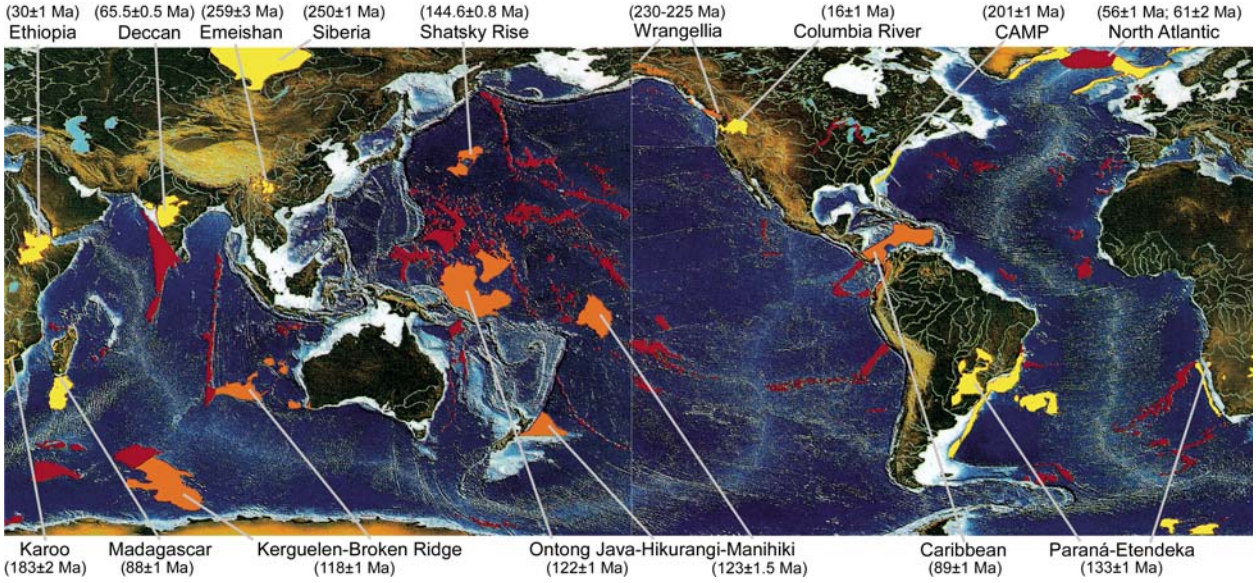

Figure 1. Map showing the distribution of Phanerozoic large igneous provinces (Mahoney and Coffin, 1997). Transient LIPs (large igneous provinces) are indicated in yellow (continental) and orange (oceanic) with peak eruption ages. Red areas are flood basalts and ocean islands. Major oceanic plateaus and flood basalts are mostly concentrated in the western Pacific and Indian Oceans. Map modified from base map by A. Goodlife and F. Martinez (*in* Mahoney and Coffin, 1997). The peak eruption ages of each LIP are from the compiled references in Courtillot and Renne (2003) and Taylor (2006). Shatsky Rise age from Mahoney et al. (2005). CAMP—Central Atlantic Magmatic Province.

Oceanic plateaus form near spreading ridges, extinct arcs, fragments of continental crust, and in intraplate settings. They form crustal emplacements 20–40 km thick with flood basalt sequences as much as 6 km thick, with individual plateaus extending as much as 2 million km^2 in area (e.g., Ontong Java Plateau; Coffin and Eldholm, 1994). Current understanding of the construction of oceanic plateaus is based on the age, composition, and stratigraphy of the volcanic rock in conjunction with observations of interrelationships between sedimentation, erosion, and magmatism (Saunders et al., 2007). Stratigraphic and geochronological studies of an obducted oceanic plateau, where the base and top of the volcanic stratigraphy are exposed, as well as the underlying and overlying sediments, provide a means for evaluating the construction of an oceanic plateau (e.g., emplacement of flows, eruption environment, tectonic setting during formation, time scale of volcanism, paleoenvironment preceding and following eruption, uplift and subsidence history).

Wrangellia flood basalts represent one of the best-exposed accreted oceanic plateaus on Earth. Wrangellia is a rare example of an accreted oceanic plateau where parts of the entire volcanic stratigraphy are exposed, as well as the prevolcanic and postvolcanic stratigraphy. This oceanic plateau is exposed in numerous fault-bound blocks in a belt extending from Vancouver Island, British Columbia, to south-central Alaska. In this contribution we integrate new observations on the volcanic stratigraphy and prevolcanic and postvolcanic stratigraphy of Wrangellia with previously published data, including geochronology and biostratigraphy, to evaluate the construction and age of the Wrangellia oceanic plateau. This material is presented as descriptions of Wrangellia stratigraphy, compiled geologic maps, photographic databases, an interactive Google Earth file, and a review and compilation of previous research on Wrangellia. The maps, photographs, and archiving of information offer tools to visualize and fully explore the large body of information about Wrangellia, bringing together past and present research to provide an overview of the architecture of the Wrangellia oceanic plateau (Greene et al., 2008, 2009a, 2009b). This contribution highlights the prominent geologic features of the Wrangellia oceanic plateau, and compares them to other oceanic plateaus, to provide information that can be used to test and refine models on the genesis of oceanic plateaus.

WRANGELLIA FLOOD BASALTS: THE VOLCANIC STRATIGRAPHY OF AN OCEANIC PLATEAU

A large part of Wrangellia formed as an oceanic plateau, or transient LIP, that accreted to western North America. Wrangellia flood basalts are the defining unit of Wrangellia, in conjunction with underlying and overlying Triassic sediments with age-diagnostic fossils (Jones et al., 1977). The flood basalts are defined as the Karmutsen Formation on Vancouver Island and the Queen Charlotte Islands (Haida Gwaii), and the Nikolai Formation in southwest Yukon and south-central Alaska (Fig. 2). Smaller elements of Middle to Late Triassic basalt stratigraphy in southeast Alaska are also believed to correlate with the Wrangellia flood basalts (Plafker and Hudson, 1980).

Geographic Distribution and Aerial Extent of the Wrangellia Flood Basalts

The Wrangellia flood basalts in British Columbia, Yukon, and Alaska have been identified by geologic mapping and regional geophysical surveys. Exposures of Wrangellia flood basalts extend ~2300 km from Vancouver Island to south-central Alaska (Fig. 2; Supplemental Google Earth File[1]). Exposures of the Karmutsen Formation cover ~58% of Vancouver Island, British Columbia. In southern Alaska, elements of Wrangellia have a well-defined northern boundary along the Denali fault and extend southward to the outboard Peninsular terrane (Fig. 2). In southeast Alaska and southwest Yukon, Wrangellia is mostly limited to slivers of intensely dissected crustal fragments with minimal aerial extent (Fig. 2).

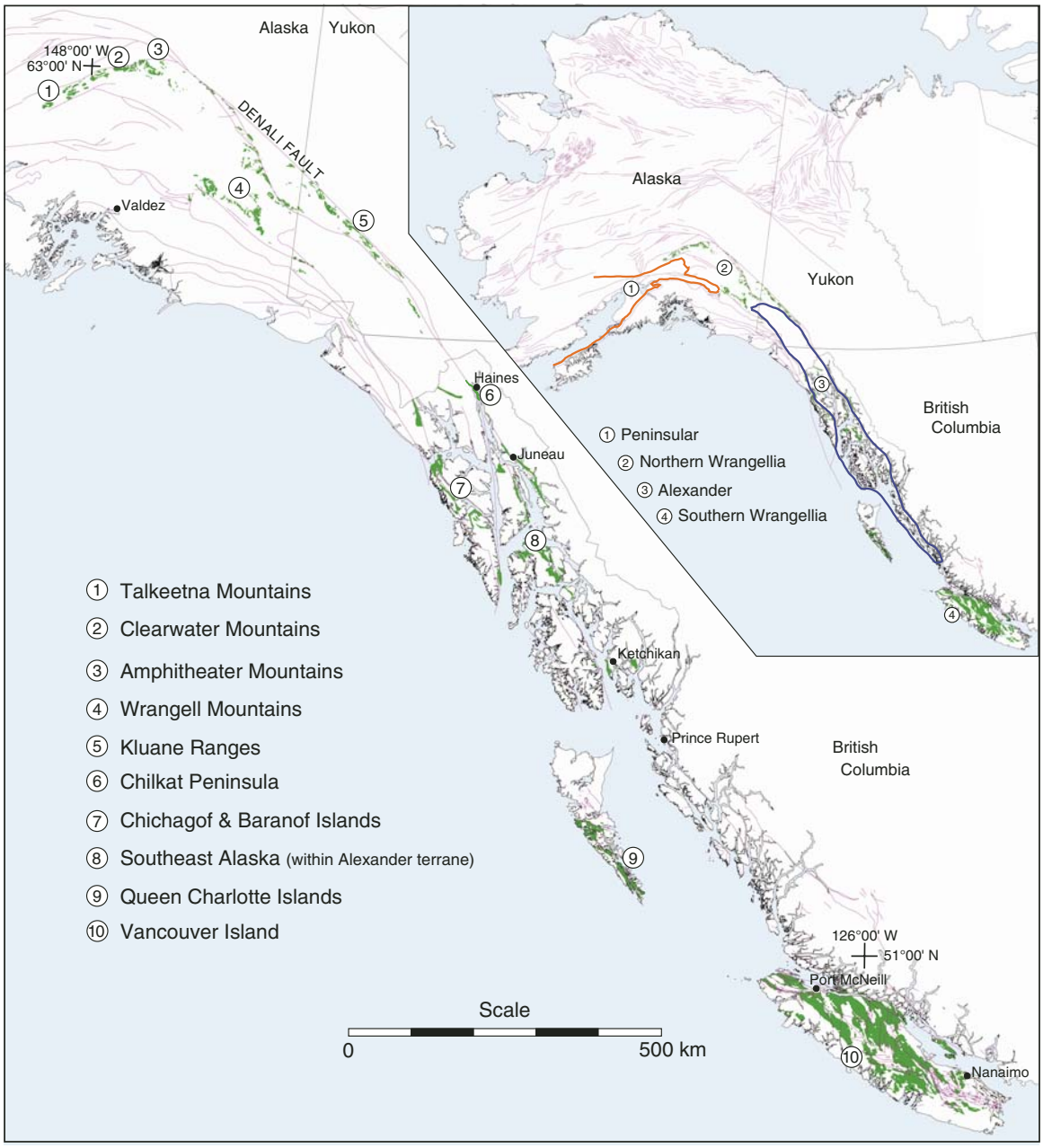

Figure 2. Simplified map showing the distribution of Wrangellia flood basalts in Alaska, Yukon, and British Columbia (green). Basalts indicated in southeast Alaska are mostly part of the Alexander terrane. Map derived from Wilson et al. (1998), Israel (2004), Massey et al. (2005a, 2005b), Wilson et al. (2005), and D. Brew (2007, written commun.). Inset shows northwest North America with Wrangellia flood basalts, and outlines for the Peninsular (orange) and Alexander (blue) terranes. Purple lines are faults in Alaska and parts of Yukon. Circled numbers indicated in the legend refer to areas mentioned in the text.

[1]Supplemental Google Earth File. ALL Wrangellia files. This .kmz file consists of georeferenced information that is designed to be viewed with the satellite imagery in Google Earth. The Google Earth application is available for free download at http://earth.google.com/. Information about Google Earth can be found at this web address. Please use the most current version of Google Earth for viewing these files (version 5.0 as of June 2009). The Supplemental Google Earth File contains ten separate folders: (1) Mapped Wrangellia flood basalts. This is a red transparent layer that shows the distribution of the Wrangellia flood basalts in Alaska, Yukon, and British Columbia. The map was derived from data in Wilson et al. (1998, 2005), Israel (2004), Massey et al. (2005a, b), and D. Brew (2007, written commun.). (2) Major faults in Alaska and Yukon. (3) Major faults in southwest BC. These folders show the location of faults in parts of Alaska, Yukon, and BC. These files were filtered from original files found at the following locations: Alaska from http://www.asgdc.state.ak.us/; Yukon from in Israel (2004); BC faults from Massey et al. (2005a, b). (4) Alaska sample locations. (5) Yukon sample locations. (6) Vancouver Island sample locations. These files show the locations, sample numbers, and flow type of samples of Wrangellia flood basalts collected during field work. (7) Alaska Range photograph locations. (8) Wrangell Mountains photograph locations. (9) Yukon photograph locations. (10) Vancouver Island photograph locations. These four folders contain small versions of georeferenced photographs. Multiple photographs are referenced to a single coordinate. Therefore, in order to view all of the photographs from a single coordinate it is necessary to open the subfolders for each region in the My Places menu so individual photographs can be selected and viewed. Zooming in also helps to distinguish photograph locations. These photographs and others can be viewed in higher resolution online at the following link: http://www.eos.ubc.ca/research/wrangellia/. If you are viewing the PDF of this paper or reading it offline, please visit http://dx.doi.org/10.1130/GES00212.S1 or the full-text article on www.gsapubs.org to view the Supplemental Google Earth File.

From recently compiled digital geologic maps, the aerial exposure of the Wrangellia flood basalts is ~20 × 10^3 km^2 on Vancouver Island, ~800 km^2 in southwest Yukon and southeast Alaska, and ~2000 km^2 across southern Alaska (Table 1). The original areal distribution was considerably greater, and these estimates of outcrop extent do not consider areas of flood basalt covered by younger strata and surficial deposits. The boundaries and crustal structure of Wrangellia in southern Alaska, as defined by recent magnetic and gravity surveys, indicate a distinct magnetic high interpreted as an expression of the presence of thick dense crust from Triassic mafic magmatism (Glen et al., 2007a, 2007b; Saltus et al., 2007). Wrangellia crust beneath Vancouver Island (~25–30 km thick) has seismic properties corresponding to mafic plutonic rocks extending to depth that are underlain by a strongly reflective zone of high velocity and density (Clowes et al., 1995). This reflective zone was interpreted by Clowes et al. (1995) as a major shear zone where lower Wrangellia lithosphere was detached.

Geologic History of Wrangellia

In this paper Wrangellia (or the Wrangellia terrane) refers to fault-bound sections of the upper crust that contain diagnostic successions of Middle to Late Triassic flood basalts and Triassic sedimentary strata that overlie Paleozoic units (as originally defined by Jones et al., 1977). The areas of Wrangellia in Alaska and Yukon are referred to as Northern Wrangellia and areas in British Columbia are referred to as Southern Wrangellia. The Wrangellia composite terrane refers to three distinct terranes (Wrangellia, Alexander, Peninsular; Fig. 2) that share similar elements or have a linked geologic history (as defined by Plafker et al., 1989, 1994; Nokleberg et al., 1994; Plafker and Berg, 1994). The connections between the Wrangellia, Alexander, and Peninsular terranes are not well established, although a single Pennsylvanian pluton in Alaska is proposed to link the Proterozoic–Triassic Alexander terrane to Wrangellia by the late Pennsylvanian (Gardner et al., 1988). This paper specifically focuses on Wrangellia and does not examine the relationship of Wrangellia to the Alexander and Peninsular terranes.

Wrangellia has a geologic history spanning a large part of the Phanerozoic prior to its accretion with western North America. The geologic record beneath the flood basalts comprises Paleozoic oceanic arc and sedimentary sequences with a rich marine fossil assemblage. Paleontological studies indicate that Southern Wrangellia was located in cool-temperate waters at northern paleolatitudes (~25°N) and not far from the North American continent during the Pennsylvanian–Early Permian (Katvala and Henderson, 2002). The geologic record is sparse to absent during the Middle Permian–Early Triassic throughout Wrangellia. A major, short-lived phase of tholeiitic flood volcanism occurred in the Middle to Late Triassic in submarine and subaerial environments. Paleomagnetic studies of Wrangellia flood basalts indicate eruption in equatorial latitudes (Irving and Yole, 1972; Hillhouse, 1977; Hillhouse and Gromme, 1984), and Late Triassic bivalves indicate an eastern Panthalassan position in the Late Triassic (Newton, 1983). A mantle plume origin for the Wrangellia flood basalts was proposed by Richards et al. (1991) and is supported by ongoing geochemical and petrological studies (Greene et al., 2008, 2009a, 2009b). Late Triassic–Early Jurassic arc magmatism is preserved as intrusions within and volcanic sequences overlying Wrangellia flood basalts throughout areas on Vancouver Island. Paleobiogeographic studies indicate that Wrangellia was located in the northeast Pacific Ocean during the Early Jurassic (Smith, 2006). Wrangellia probably accreted to western North America in the Late Jurassic–Early Cretaceous (e.g., Csejtey et al., 1982; McClelland et al., 1992; Nokleberg et al., 1994; Umhoefer and Blakey, 2006; Trop and Ridgway, 2007), and was caught up in the Cretaceous–Eocene thermal events of the Coast Mountains, as well as partly covered by younger sediments (Hollister and Andronicos, 2006).

SUMMARY OF THE STRATIGRAPHY OF WRANGELLIA

A full description of prominent features of Wrangellia stratigraphy and a summary of previous research are presented in the supplemental figure, map, methods, and data files. Table 2 provides a synthesis of Wrangellia stratigraphy. Supplementary Data Files 1[2] and 2[3] also contain a compilation of ~500 references related to Wrangellia.

TABLE 1. AREAL EXTENT AND VOLUMETRIC ESTIMATES FOR THE WRANGELLIA FLOOD BASALTS

Region and/or quadrangle	Area (km^2)	Area (%)	Estimated thickness (km)		Estimated volume (km^3)		Rel. volume (%)
			minimum	maximum	minimum	maximum	
British Columbia							
Southern VI (NM10)	10,581	41.9	4	6	42,323	63,485	45.2
Northern VI (NM9)	8,561	33.9	4	6	34,245	51,368	36.6
Queen Charlotte Is (NN8)	1,773	7.0	3	4.5	5,319	7,979	5.7
Queen Charlotte Is (NN9)	1,827	7.2	3	4.5	5,481	8,221	5.9
Northern BC (NO8)	86	0.3	1	3	86	257	0.2
Yukon							
Kluane South	705	2.8	1	3	705	2,115	1.5
Alaska							
McCarthy	720	2.9	3	4	2,161	2,882	2.1
Nabesna	275	1.1	3	4	824	1,098	0.8
Valdez	55	0.2	1	2	55	110	0.1
Gulkana	7	0.0	1	2	7	14	0.0
Mt Hayes	356	1.4	3	4.5	1,067	1,601	1.1
Healy	205	0.8	3	4.5	616	924	0.7
Talkeetna Mtns	105	0.4	3	4.5	314	471	0.3
Total	25,256				93,204	140,525	

Note: Area estimates for British Columbia are calculated from Massey et al. (2005). Area estimates for Yukon are calculated from Israel et al. (2004). Area estimates for Alaska are calculated from Wilson et al. (1998, 2005). Rel.—relative; VI—Vancouver Island; BC—British Columbia; Is—Island; Mtns—mountains.

TABLE 2. STRATIGRAPHY OF WRANGELLIA

Vancouver Island	Alaska Range, Alaska	Wrangell Mountains, Alaska and Kluane Ranges, Yukon
(up to Jurassic listed)	*(minor sediments overlying Nikolai Fm. are preserved)*	*(up to Jurassic listed)*
LeMare Lake Volcanics and Bonanza Volcanics		Root Glacier Fm. (1200 m; shale, ss, conglomerate)
Subaerial basalt and rhyolite flows, breccia, tuff	Clearwater Mtns.	Lube Creek Fm. (90 m; chert, coquina)
Waterlain pyroclastics (Island Plutonic Suite)	Argillite with calcareous horizons, minor volcanic rocks	
Minor pillow lava, hyaloclastite, epiclastic deposits	Minor conglomerate, local limestone	McCarthy Fm. (~1000 m; Late Triassic–Early Cretaceous)
Parson Bay Formation (300–600 m)	Diagnostic Late Triassic index fossils	Shale, chert, limestone, minor tuff beds
Well-bedded shale, limestone, minor volcanics	(bivalve *Halobia* and ammonoid *Tropites*)	Nizina Fm. (100–375 m; Late Triassic)
Quatsino Formation (40–500 m)		Thinly bedded limestone, chert
Massive to well-bedded micritic limestone		Chitistone Fm. (375-630 m; Late Triassic)
(local bioclastic limestone, local intra-Karmutsen limestone)	*(above Wrangellia flood basalts)*	(local intra-Nikolai limestone)
Karmutsen Formation (~6000 m; Middle to Late Triassic)	Nikolai Formation (~3500 m; Middle to Late Triassic)	Nikolai Formation (~3500 m; Middle to Late Triassic)
Subaerial basalt flows (minor pillow basalt and/or breccia)	Subaerial basalt flows (~3000 m)	Subaerial basalt flows
(>2500 m on CVI, <1500 m on NVI)	Minor tuff and flow breccia	3.5 km thick in Wrangell Mtns.
Pillow breccia and hyaloclastite (400–1500 m on NVI)	Pillowed submarine flows(<800 m; small-diameter pillows)	1 km thick in Kluane Ranges, intensely faulted
Keogh Lake picrite (pillow lavas, NVI)		Flow conglomerate, pillow breccia along base (<100 m)
Pillowed and massive submarine flows (2000–3000 m)	Minor picritic pillow lavas	
	(below base of Wrangellia flood basalts)	
(Central Vancouver Island)		
Middle Triassic Daonella beds and mafic sills (~1000 m)	Middle Triassic nonfossiliferous black shale	Middle Triassic Daonella beds and mafic intrusive rocks
Silicified shale, chert, minor limestone	Intruded by mafic sills related to Nikolai Fm. (<300 m)	
Buttle Lake Group (~2000 m; Mississippian–Early Permian)	Eagle Creek Fm. (~900 m; Early Permian)	Skolai Group
Massive bioclastic limestone (Mount Mark Fm.)	Argillite and limestone	Golden Horn Limestone Lentil (varies, locally ~250 m)
Argillite with interbedded limestone (Fourth Lake Fm.)	Mafic and ultramafic intrusives related to Nikolai Fm.	Richly bioclastic limestone (Early Permian)
Minor conglomerate	Slana Spur Fm. (~1400 m; Penn.–Early Permian)	Crinoid stems, bryozoans, brachiopods, corals
	Marine calcareous volcanic rocks, sandstone,	Hasen Creek Fm. (locally ~300 m; Permian)
Sicker Group (~3000 m; Devonian–Early Mississippian)	and conglomerate	Chert, shale, limestone, local mafic intrusives
Primarily arc-derived volcanic rocks	Tetelna volcanics (~1000 m; Pennsylvanian)	Station Creek Fm. (~2000–2500 m; Penn.–Early Permian)
Andesitic flows, pillow basalt, flow breccia, tuffs	Andesitic flows, volcanic breccia, conglomerate	Arc-derived volcanic rocks
Tuffaceous and cherty sediments		Upper volcaniclastic member (~800 m)
Mafic sills and intrusive suites	Large mafic and/or ultramafic intrusions related to Nikolai Fm.	Lower volcanic flow member (~1200 m)
	Within Paleozoic basement	
(deepest level of exposure)	*(deepest level of exposure)*	*(deepest level of exposure)*

Note: See supplementary data files for list of references. NVI, CVI—Northern and Central Vancouver Island, Penn.—Pennsylvanian, Mts.—mountains, ss—sandstone, Fm.—formation. Italicized text—notes about stratigraphic column.

[2]Supplemental Data File 1. Endnote database for Wrangellia. This Endnote library is a compilation of approximately 500 references mostly related to research of Wrangellia or parts of western North America. This is a zipped file containing an .enl database file and a folder named SD1_Endnote_database_Wrangellia.Data, which is needed to open the .enl file. The .enl file was created with Endnote X1.0.1 (Bld 2682) and should be compatible with older versions of Endnote. If you are viewing the PDF of this paper or reading it offline, please visit http://dx.doi.org/10.1130/GES00212.S2 or the full-text article on www.gsapubs.org to view Supplemental Data File 1.

[3]Supplemental Data File 2. Reference list for Wrangellia. This Microsoft Word file is an exported version of the Endnote file in Supplemental Data File 1. If you are viewing the PDF of this paper or reading it offline, please visit http://dx.doi.org/10.1130/GES00212.S3 or the full-text article on www.gsapubs.org to view Supplemental Data File 2.

Northern Wrangellia

The accretion and northward tectonic migration of parts of Wrangellia, followed by the oroclinal bending of Alaska, has left Wrangellia flood basalts exposed in an arcuate belt extending ~450 km across south-central Alaska (Fig. 3). Wrangellia stratigraphy forms most of the Wrangell Mountains in the eastern part of southern Alaska and extends westward in a wide belt immediately south of the Denali fault, along the southern flank of the eastern Alaska Range and in the northern Talkeetna Mountains (Fig. 3). The northwestern boundary of Wrangellia corresponds with a prominent steeply dipping structure (Talkeetna suture zone), which may represent the original suture between Wrangellia and the former continental margin (Glen et al., 2007a). Mesozoic and Cenozoic sedimentary basins along the inboard margin of Wrangellia, adjacent to and overlying the Talkeetna suture zone and Denali fault, record the uplift and collisional history of Wrangellia and the former continental margin, north of the Denali fault (Trop et al., 2002; Ridgway et al., 2002; Trop and Ridgway, 2007).

Some of the best exposures of Wrangellia flood basalt stratigraphy are preserved as part of an east-west–trending synform underlain by mafic and ultramafic plutonic rocks in the Amphitheater Mountains (Figs. 3 and 4). There are ~3 km of subaerial basalt flows overlying <800 m of submarine stratigraphy in the Amphitheater Mountains. Wrangellia flood basalts also form two prominent northwest- to southeast-trending belts along the northeast and southwest margins of the Wrangell Mountains, between the Totschunda fault and Chitina thrust belt (Fig. 3). The Nikolai Formation in the Wrangell Mountains is estimated to be ~3.5 km in total thickness and is composed almost entirely of subaerial flows (MacKevett, 1978). The Nikolai Formation consists of low-titanium basalts that form the lowest ~400 m of volcanic stratigraphy in the Alaska Range, and the remainder of the volcanic stratigraphy in the Alaska Range and all of the sampled stratigraphy in the Wrangell Mountains are high-titanium basalt (Greene et al., 2008). A cumulative thickness of >3.5 km of marine sedimentary rocks, which range in age from Late Triassic to Late Jurassic, overlies the Nikolai basalts in the Wrangell Mountains. From the Nutzotin Mountains along the Alaska-Yukon border to southeast Alaska, Wrangellia forms a thin northwest- to southeast-trending belt in the southwest corner of Yukon (Fig. 2). The best exposures of Wrangellia in Yukon are in the Kluane Ranges, where the stratigraphy is similar in most aspects to stratigraphy in the Wrangell Mountains, and it has been described using the same nomenclature (Muller, 1967; Read and Monger, 1976). Triassic basaltic and sedimentary rocks with similarities to Wrangellia sequences in southern Alaska are exposed as elongate fault-bound slivers within a large and complex fault system in the Alexander terrane in several areas of southeast Alaska.

Southern Wrangellia

Northern and central Vancouver Island is underlain by Wrangellia, which forms the uppermost sheet of a thick sequence of northeast-dipping thrust sheets that constitute the upper crust of Vancouver Island (Fig. 5; Monger and Journeay, 1994; Yorath et al., 1999). Wrangellia lies in fault contact with the Pacific Rim terrane and Westcoast Crystalline Complex to the west, and is intruded by the predominantly Cretaceous Coast Plutonic Complex to the east (Wheeler and McFeely, 1991). The cumulative thickness of Wrangellia stratigraphy exposed on Vancouver Island is >10 km (Yorath et al., 1999). Two prominent northwest- to southeast-trending anticlinoria (Buttle Lake and Cowichan) are cored by Paleozoic rocks, which are not exposed on northern Vancouver Island (Fig. 5; Brandon et al., 1986; Yorath et al., 1999). Wrangellia also forms a large part of the southern Queen Charlotte Islands, where it is mostly unsampled.

The deepest stratigraphic levels of Wrangellia, which are exposed in the Buttle Lake and Cowichan anticlinoria, comprise the lower to middle Paleozoic Sicker Group and the upper Paleozoic Buttle Lake Group (Fig. 5). The combined total thickness of the Sicker and Buttle Lake Groups is estimated to be ~5000 m (Massey, 1995; Yorath et al., 1999; Fig. 5).The basalt stratigraphy around Buttle Lake is proposed as the type section for the Karmutsen Formation, as this is where the most complete stratigraphic section is preserved (~6 km thick; Figs. 5 and 6; Yorath et al., 1999). Recent mapping on northern Vancouver Island has delineated the three-part volcanic stratigraphy of pillowed lava sequences, hyaloclastite, and subaerial flows of the Karmutsen Formation (Fig. 6; Greene et al., 2009b; Nixon et al., 2008). Picritic pillow basalts occur near the top of the submarine basalt stratigraphy on northern Vancouver Island (Greene et al., 2006, 2009b). A photographic archive of field relationships in Wrangellia is available as an abbreviated version in the Supplemental Figure File[4] and in full online at http://www.eos.ubc.ca/research/wrangellia/. Additional geologic maps for areas of Alaska, Yukon, and Vancouver Island can be found in the Supplemental Map File[5].

AGE OF WRANGELLIA FLOOD BASALTS

Previous Geochronology for Wrangellia Flood Basalts and Related Plutonic Rocks

Samples of Wrangellia flood basalts and related plutonic rocks from British Columbia, Yukon, and Alaska were previously dated in eight separate studies; these results are summarized in Table 3 (all ages below are quoted with 2σ analytical uncertainty). A total of 15 ages (4 U-Pb, 9 $^{40}Ar/^{39}Ar$, and 2 K-Ar) from the literature include 4 basalts and 11 plutonic rocks. In Southern Wrangellia, 3 U-Pb ages from gabbroic rocks on southern Vancouver Island are available, including (1) a single concordant analysis of a multigrain baddeleyite fraction that yielded a $^{206}Pb/^{238}U$ age of 227.3 ± 2.6 Ma (Parrish and McNicoll, 1992), and (2) two unpublished $^{206}Pb/^{238}U$ baddeleyite ages of 226.8 ± 0.5 Ma (5 fractions) and 228.4 ± 2.5 (2 fractions) (Table 2; Sluggett, 2003). A single whole rock of Karmutsen basalt from Buttle Lake on Vancouver Island yielded a $^{40}Ar/^{39}Ar$ plateau age of 224.9 ± 13.2 Ma (Lassiter, 1995).

In Northern Wrangellia, the U-Pb results for zircon separated from a gabbro sill possibly related to the Nikolai basalts in southwest

[4]Supplemental Figure File. This PDF file contains nine figures with captions. These figures accompany Supplemental Data File 7 and illustrate some of the exceptional exposures of the volcanic stratigraphy of the Wrangellia plateau in Alaska, Yukon, and British Columbia. Additional georeferenced photographs are part of the Supplemental Google Earth File and also can be found at the following website dedicated to research on Wrangellia: http://www.eos.ubc.ca/research/wrangellia/. If you are viewing the PDF of this paper or reading it offline, please visit http://dx.doi.org/10.1130/GES00212.S4 or the full-text article on www.gsapubs.org to view the Supplemental Figure File.

[5]Supplemental Map File. This file contains four maps of different parts of Wrangellia in a single pdf file with references. Two maps are simplified regional geologic maps of southwest Yukon and southeast Alaska showing the distribution of Triassic flood basalts. Two maps are detailed geologic maps of areas in the Amphitheater Mountains in the Alaska Range and on northern Vancouver Island. If you are viewing the PDF of this paper or reading it offline, please visit http://dx.doi.org/10.1130/GES00212.S5 or the full-text article on www.gsapubs.org to view the Supplemental Map File.

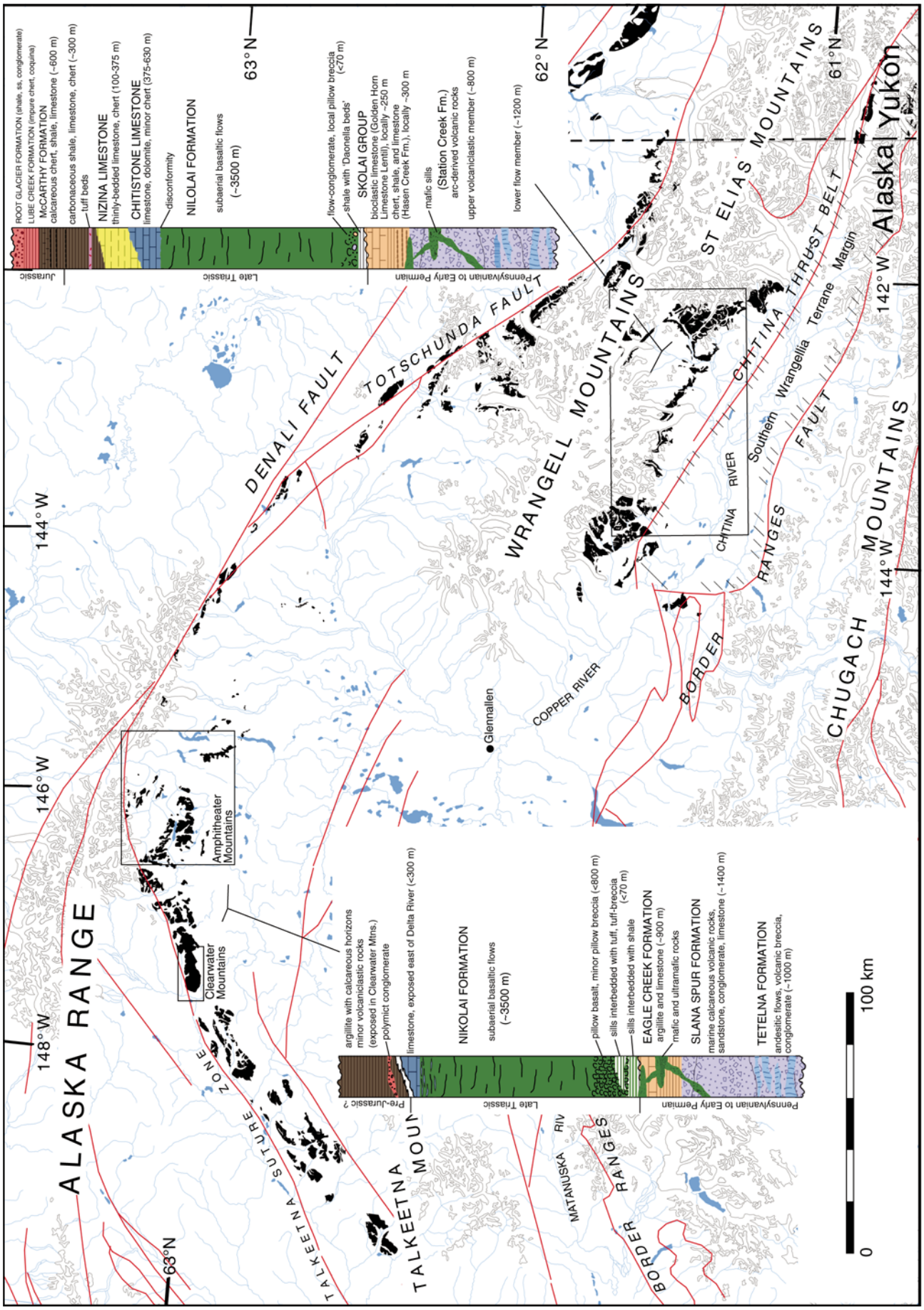

Figure 3. Simplified map of eastern south-central Alaska showing the distribution of Wrangellia flood basalts (black) and stratigraphic columns. Map is derived from Wilson et al. (1998) and Wilson et al. (2005), with mapping from Schmidt et al. (2003b). Stratigraphic columns depict late Paleozoic–Jurassic units on the south side of the Wrangell Mountains (derived from Smith and MacKevett, 1970; MacKevett, 1978), and the east-central Alaska Range (derived partly from Nokleberg et al., 1992). Fm—Formation; ss—sandstone.

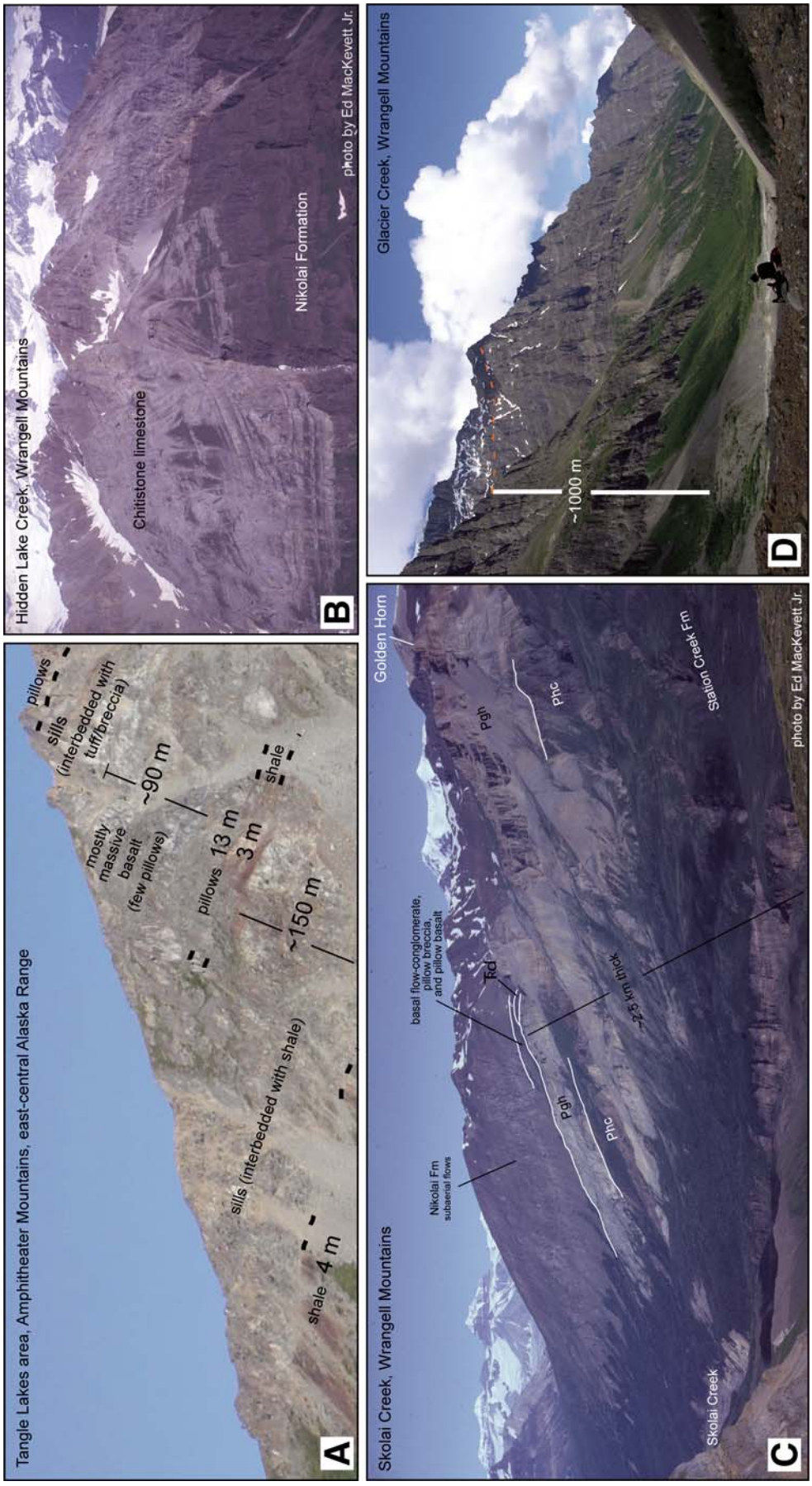

Figure 4. Photographs of the base of the Nikolai Formation in the Alaska Range and Wrangell Mountains, Alaska (locations shown in Fig. 3). (A) Sediment-sill complex and base of flood basalts on the west side of Lower Tangle Lake. (B) Photograph of the top of the Nikolai Formation and overlying Chitistone Limestone (taken by Ed MacKevett, Jr.). Several faults offset the contact. (C) Paleozoic arc rocks and marine sedimentary sequences underlying Nikolai basalts. Photograph by Ed MacKevett, Jr. (Phc—Hasen Creek Formation; Pgh—Golden Horn Limestone Lentil; TRd—Middle Triassic *Daonella* beds). (D) Photograph of ~1000 m of subaerial basalt flows overlain by Chitistone Limestone (dashed orange line indicates the contact).

Yukon yielded an age of 232.2 ± 1.0 Ma (average $^{207}Pb/^{206}Pb$ age of 3 discordant [1.6%–2.4%] analyses from multigrain zircon fractions) (Table 3; Mortensen and Hulbert, 1991). K-Ar dating of biotite from peridotite in the Kluane mafic-ultramafic complex provided ages of 224 ± 8 Ma and 225 ± 7 Ma (Campbell, 1981). In Alaska, three samples of Wrangellia flood basalts from the Wrangell Mountains yielded whole rock $^{40}Ar/^{39}Ar$ plateau ages of 228.3 ± 5.2 Ma, 232.8 ± 11.5 Ma, and 232.4 ± 11.9 Ma (Lassiter, 1995). Five $^{40}Ar/^{39}Ar$ plateau and isochron ages of variable precision have been determined for hornblende and biotite separates from mafic and ultramafic plutonic rocks in the Amphitheater Mountains in the Alaska Range (Table 3). Three of these samples, with ages of 225.2 ± 6.5 Ma, 225.7 ± 2 Ma, and 228.3 ± 1.1 Ma, are from the Rainy Creek area, which is to the north across a major fault from typical volcanic stratigraphy of Wrangellia flood basalts (Bittenbender et al., 2007). The Rainy Creek area is a steeply dipping sequence of picritic tuff and volcaniclastic rocks, mafic and ultramafic intrusive rocks and dikes, and limestone that is distinct from the stratigraphy of the Nikolai Formation; these units may be older than the Wrangellia flood basalts (Bittenbender et al., 2003) or may be younger (Nokleberg et al., 1992). Two gabbros related to Wrangellia flood basalts in the Tangle Lakes area of the Amphitheater Mountains have reported $^{40}Ar/^{39}Ar$ ages of 230.4 ± 2.3 and 231.1 ± 11 Ma (Bittenbender et al., 2003; Schmidt and Rogers, 2007); however, analytical information is not available for these samples.

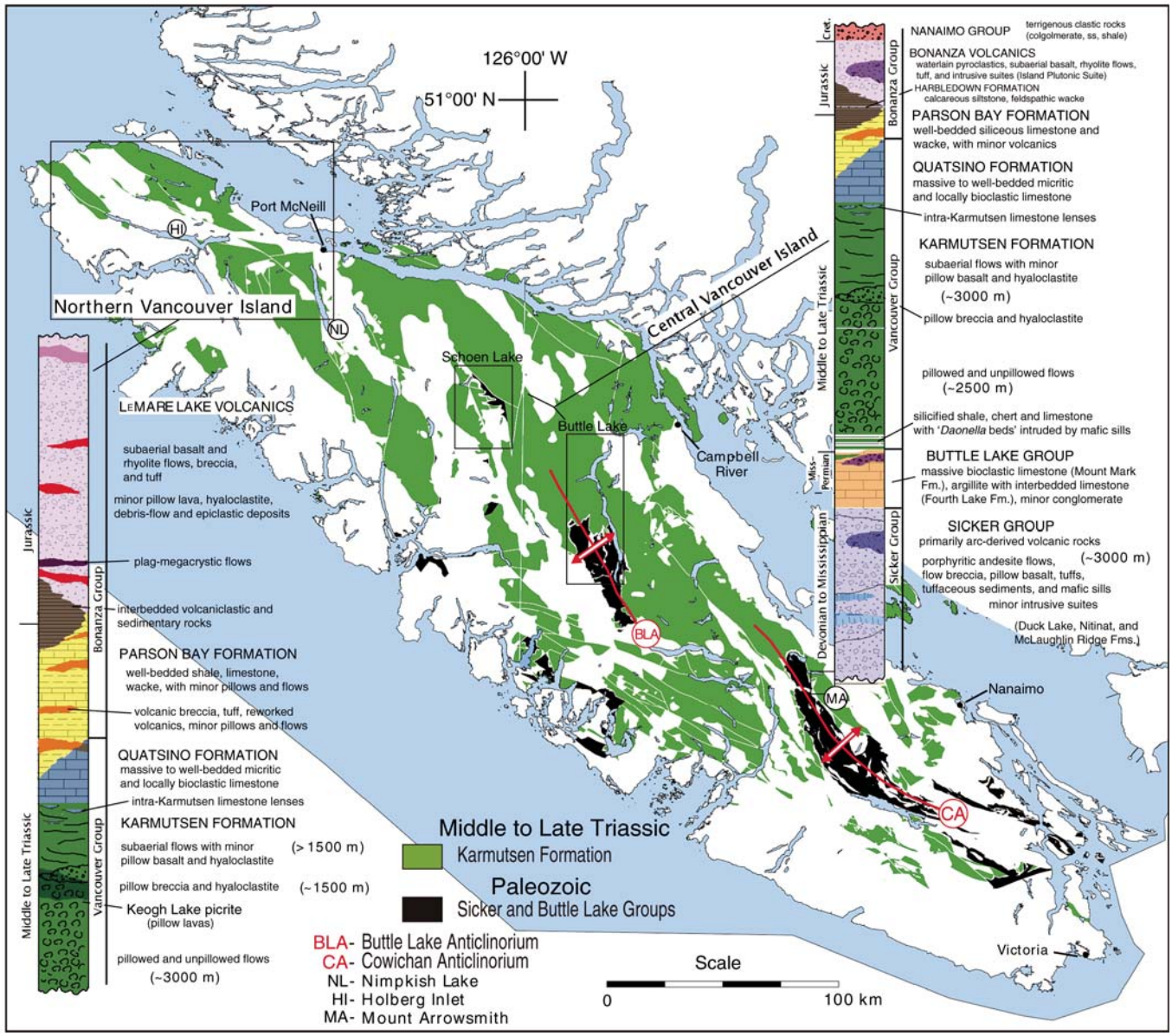

Figure 5. Simplified map of Vancouver Island, British Columbia, showing the distribution of the Karmutsen Formation (green) and underlying Paleozoic formations (black) (after Massey et al., 2005a, 2005b). The main areas of field study are indicated with boxes or circles with uppercase letters (see legend). Stratigraphic columns are shown for northern and central Vancouver Island. Column for northern Vancouver Island is adapted from Nixon and Orr (2007). Column for central Vancouver Island is derived from Carlisle (1972), Juras (1987), Massey (1995), and from field work. Fm.—Formation; ss—sandstone. Red lines indicate the axes of anticlinoria.

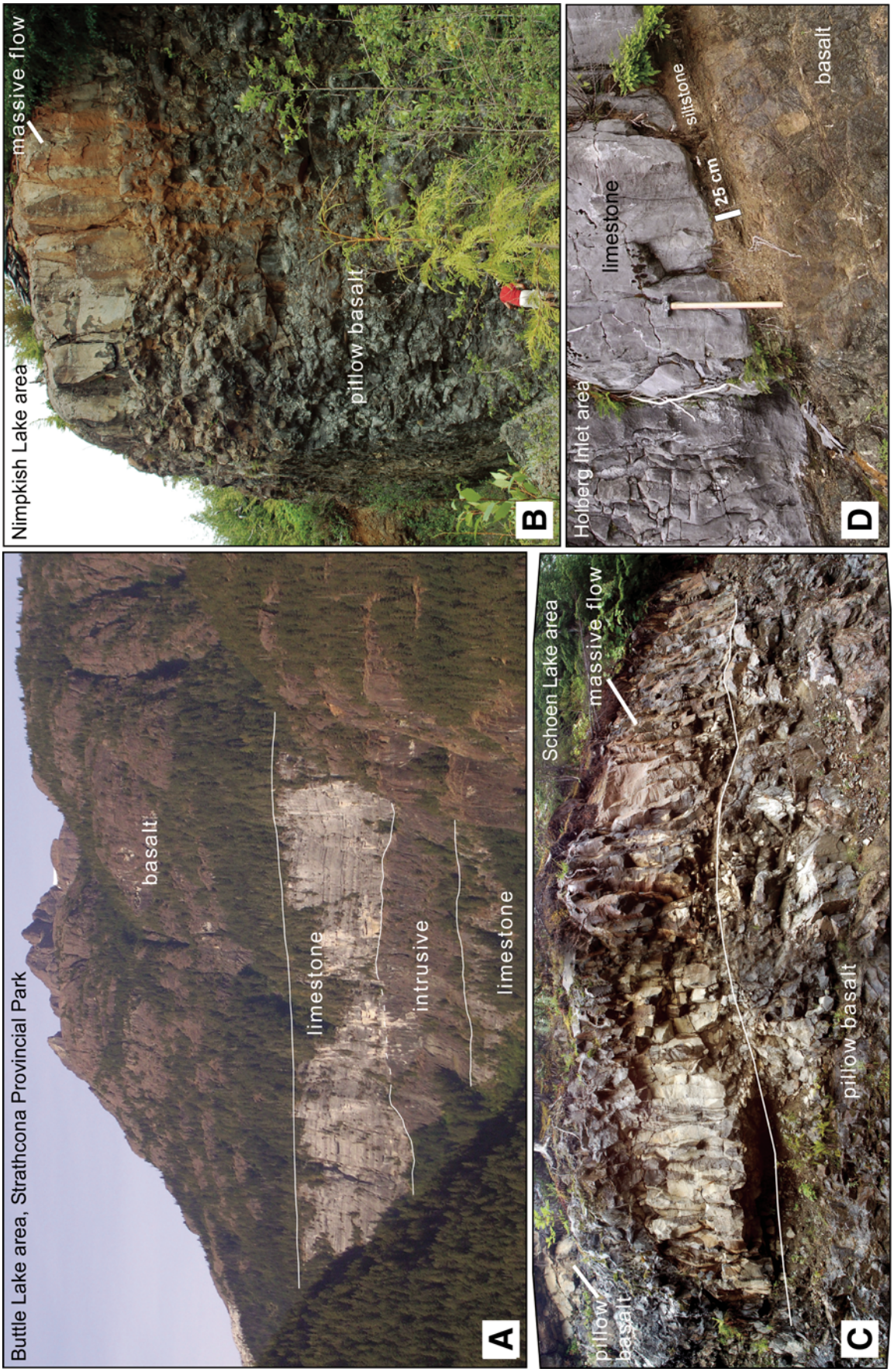

Figure 6. Field photographs of the Karmutsen Formation on Vancouver Island (locations shown in Fig. 5). (A) Photograph of contact between limestone of the upper Paleozoic Buttle Lake Group intruded by mafic sills, related to Karmutsen basalts, and overlain by pillow basalt of the Karmutsen Formation. (B) Photograph of massive submarine flow draped over thick sequence of pillow basalt in the Alice-Nimpkish Lake area. (C) Photograph of a massive submarine flow with hackly jointing surrounded by pillow basalt in the Schoen Lake area. (D) Photograph of contact between top of the Karmutsen Formation and overlying Quatsino limestone.

TABLE 3. COMPILATION OF PREVIOUSLY PUBLISHED GEOCHRONOLOGY OF WRANGELLIA FLOOD BASALTS AND ASSOCIATED PLUTONIC ROCKS

Sample number	Age	Error ± 2σ	Method	Material	Reference	Rock description and location	Comment
Alaska Range							
00AG022	231.1	11	Ar-Ar	Hornblende	Schmidt and Rogers, 2007	Gabbro; Tangle Lakes area, southwestern Grizzly Ridge	Total fusion age. No analytical information available. Analysis by L. Snee (USGS). 62.7°N, 148.5°W
PB1	230.4	2.3	Ar-Ar	Biotite	Bittenbender et al., 2003†	Gabbro; Tangle Lakes area	No analytical information available
AK25515	228.3	2.2	Ar-Ar	Biotite	Bittenbender et al., 2007†	Gabbro with poikilitic biotite, including olivine; Rainy Creek Complex	Plateau age, 5 fractions, 81% of ^{39}Ar released, integrated age: 226.0 ± 1.1 Ma; interpreted as age of magmatism
HBD-2003-29	225.7	4	Ar-Ar	Hornblende	Bittenbender et al., 2007†	Olivine basalt; Rainy Creek Complex	Plateau age, 8 fractions, 97% of ^{39}Ar released, integrated age: 226.4 ± 2.0 Ma; Interpreted as cooling age following crystallization
10830	225.2	13	Ar-Ar	Hornblende*	Bittenbender et al., 2007†	Olivine peridotite; Rainy Creek Complex	Invserse isochron age; interpreted as an alteration age, maximum age for a reset event. Impure separate, excess Ar
Wrangell Mountains							
92LNG-19	228.3	5.2	Ar-Ar	Whole rock	Lassiter, 1995§	Nikolai basalt flow from the upper third of the volcanic stratigraphy; Glacier Creek	^{40}Ar/^{39}Ar step-heating technique; inverse isochron age: 224.8 ± 5.2 Ma; 58% of ^{39}Ar released; n = 5/7
92LNG-42	232.8	11.5	Ar-Ar	Whole rock	Lassiter, 1995§	Nikolai basalt flow, ~100 m above the base of the basalt stratigraphy; Skolai Creek	^{40}Ar/^{39}Ar step-heating technique; inverse isochron age: 230.5 ± 27.8 Ma; 57% of ^{39}Ar released; n = 4/7
92LNG-47	232.4	11.9	Ar-Ar	Whole rock	Lassiter, 1995§	Nikolai basalt flow, from the lower part of the basalt stratigraphy; Skolai Creek	^{40}Ar/^{39}Ar step-heating technique; inverse isochron age: 228.1 ± 11.8 Ma; 69% of ^{39}Ar released; n = 5/7
Yukon							
HDB88-TAT22	232.2	1	U-Pb	Zircon	Mortensen and Hulbert, 1992	Maple Creek gabbro; Kluane Ranges	Average ^{207}Pb/^{206}Pb age of 3 discordant (1.6 to 2.4%) analyses from multigrain zircon fractions
SC1	224	8	K-Ar	Biotite	Campbell, 1981	Peridotite; Tatamagouche Creek, Kluane Ranges	K-Ar age. No analytical information available. Analysis at University of British Columbia by J.E. Harakal
SC2	225	7	K-Ar	Biotite	Campbell, 1981	Peridotite; White River, Kluane Ranges	K-Ar age. No analytical information available. Analysis by M. Lanphere (USGS)
Vancouver Island							
02-CS-14	228.4	2.5	U-Pb	Zircon	Sluggett, 2003	Mount Tuam gabbro; Saltspring Island	^{206}Pb/^{238}U ages for 2 concordant fractions are 229.4 ± 2.5 and 228.4 ± 1.6 Ma. Crystallization age interpreted to be 228.4 ± 2.5 Ma
84822-1C	227.3	2.6	U-Pb	Baddeleyite	Parrish and McNicoll, 1992	Porphyritic gabbroic rock; Crofton, southern Vancouver Island	^{206}Pb/^{238}U age from a single concordant analysis of a multigrain baddeleyite fraction
02-CS-11	226.8	0.5	U-Pb	Zircon	Sluggett, 2003	Mount Tuam gabbro; Saltspring Island	^{206}Pb/^{238}U age for 1 of 5 fractions, interpreted as the crystallization age. ^{206}Pb/^{238}U ages of other fractions are 219.8 ± 0.7, 223.3 ± 0.5, 221.9 ± 0.6, and 233.9 ± 1.4 Ma, which were interpreted to indicate post-crystallization Pb-loss
91LKB-46	224.9	13.2	Ar-Ar	Whole rock	Lassiter, 1995§	Karmutsen basalt flow, Buttle Lake, central Vancouver Island	^{40}Ar/^{39}Ar step-heating technique; inverse isochron age: 213.7 ± 20.5; 69% of ^{39}Ar; n = 5/7

Note: Errors are 2σ. USGS—U.S. Geological Survey.

*Replaces clinopyroxene.

†Analyses provided courtesy of P. Bittenbender: Analyses preformed at the Geochronology Laboratory at the University of Alaska, Fairbanks. Monitor mineral MMhb-1 (Samson and Alexander, 1987) with an age of 513.9 Ma (Lanphere and Dalrymple, 2000) was used to monitor neutron flux.

§Analyses provided courtesy of R. Duncan (Oregon State University), originally interpreted in Lassiter (1995): ^{40}Ar/^{39}Ar ages are reported relative to biotite standard FCT-3 (28.03 ± 0.16 Ma, Renne et al., 1998), calculated with ArArCalc (Koppers, 2002); n = number of heating steps used/total.

$^{40}Ar/^{39}Ar$ Geochronological Results

Analytical methods for $^{40}Ar/^{39}Ar$ dating are described in Supplemental Methods File[6]. Petrographic textures and major and trace element chemistry for all of the geochronological samples are listed in Supplemental Data File 3[7]. Age spectra are shown in Figure 7 and the analytical results are summarized in Table 4; the analytical data are available in Supplemental Data File 4[8]. All ages indicated below are interpreted to represent cooling ages that correspond to the bulk closure temperature (T_{cb}) of the different minerals to Ar diffusion (~200 °C plagioclase; ~550 °C hornblende; ~350 °C biotite; as summarized in Hodges, 2003). We processed 20 mineral separates, including 14 plagioclase separates prepared from the basalt and intrusive samples, 5 hornblende separates, and 1 biotite separate, from 19 samples from throughout Wrangellia for $^{40}Ar/^{39}Ar$ dating; 13 samples were Wrangellia flood basalts or intrusive equivalents and 6 were from younger, crosscutting intrusive rocks. Of the 13 Wrangellia flood basalts or intrusive samples, 9 were basalt flows and 4 were mafic sills or gabbroic rocks. One biotite separate was from an ultramafic plutonic rock from the Kluane Ranges, Yukon (sample 05-SIS-751). The five hornblende separates were all from younger dikes and intrusions that crosscut Wrangellia basalts and were selected as they provide minimum ages for eruption. The samples that are younger crosscutting intrusive units are clearly distinguishable from the Wrangellia flood basalts by their different textures and whole-rock chemistry.

Plagioclase separates from three basalt flows (two submarine and one subaerial flow) and one gabbro from Vancouver Island were analyzed. The incremental heating data of the three basalt flows form plateaus over 67%–96% of the ^{39}Ar released with ages of 72.5 ± 1.2 Ma, 180.9 ± 3.1 Ma, and 161.1 ± 7.3 Ma (Fig. 7A; Table 4); inverse correlation diagrams ($^{39}Ar/^{40}Ar$ versus $^{36}Ar/^{40}Ar$) yield isochron ages that are concordant with the plateau ages. The results for a gabbro from the Alice–Nimpkish Lake area display a disturbed saddle-shaped age spectrum and may have been affected by excess ^{40}Ar (e.g., Lanphere and Dalrymple, 1976; Harrison and McDougall, 1981). The crosscutting mafic dike (sample 4718A3) yields a plateau age of 193 ± 26 Ma (54% of the ^{39}Ar released) and a broadly concordant isochron age of 186 ± 13 Ma (Fig. 7A; Table 4).

Plagioclase separates from five basalt flows and one mafic sill in Alaska, including two samples from the Wrangell Mountains and four samples from the Alaska Range, yield a total of three interpretable ages based on plateau ages (80%–99% of the ^{39}Ar released): 191 ± 11 Ma, 160.7 ± 1.3 Ma, and 169.0 ± 2.4 Ma (Fig. 7B; Table 4). For sample 5810A4, the plateau age (137.3 ± 8.5 Ma) is considerably younger than the integrated age (160.57 ± 8.64 Ma), reflecting the younger ages of the lower temperature steps included in the plateau age. The individual step-heating results for sample 5719A5 are associated with relatively large errors, and two samples of basalt flows (5715A1, 5810A10) show strongly disturbed $^{40}Ar/^{39}Ar$ systematics (Fig. 7B).

The biotite separate from a peridotite in Yukon yields a plateau based on results from the higher temperature steps (60% of the ^{39}Ar released), with an age of 227.5 ± 1.2 Ma and an inverse isochron age of 226.1 ± 3 Ma (Fig. 7C; Table 4). Plagioclase separates from two basalt flows from different levels of the volcanic stratigraphy of the Nikolai Formation in Yukon display strongly disturbed age spectra (Fig. 7C).

Hornblende separates from four younger intrusive samples from Alaska, including two samples from the Wrangell Mountains and two samples from the Alaska Range, yield plateau ages (54%–95% of the ^{39}Ar released) of 29.7 ± 1.1 Ma, 123.13 ± 0.77 Ma, 148.80 ± 0.83 Ma, and 149.9 ± 0.93 Ma (Fig. 7D; Table 4); the plateau ages for these samples correspond with their respective isochron ages. The results for two hornblende analyses from an amphibolite dike in the Rainy Creek area of the Amphitheater Mountains show disturbed $^{40}Ar/^{39}Ar$ systematics (Fig. 7D).

Interpretation of New $^{40}Ar/^{39}Ar$ Geochronology

Among the 13 samples of Wrangellia flood basalt that were analyzed in this study, the results for eight samples satisfy the spectra and isochron criteria to be geologically interpretable $^{40}Ar/^{39}Ar$ ages (see Supplemental Data File 4 [see footnote 8]). The only sample inferred to have retained a magmatic age is the peridotite from Yukon for which the biotite separate yields a plateau age of 227.5 ± 1.2 Ma. This age, which corresponds to cooling of the ultramafic intrusion through the T_{cb} of biotite (~350 °C) and is thus a minimum age of crystallization, is consistent with the range of previously published and reported ages from 227 to 233 Ma for emplacement of the Wrangellia flood basalts described above. The remaining seven ages from the Wrangellia basalts range from 191 to 73 Ma, indicating open-system behavior of the $^{40}Ar/^{39}Ar$ systematics (Table 4). The Karmutsen basalts on Vancouver Island underwent prehnite-pumpellyite facies metamorphic conditions (1.7 kbar, ~300 °C) and higher metamorphic gradients where proximal to granitoid intrusions (Cho and Liou, 1987), and the mineralogy of Nikolai basalts in Alaska indicates a similar degree of metamorphism. Plagioclase, which has a low T_{cb} for Ar diffusion (<200 °C; Cohen, 2004), was analyzed from each of these samples, thus these samples likely degassed ^{40}Ar during thermal resetting at some period after their emplacement.

Despite resetting, the $^{40}Ar/^{39}Ar$ ages of these basalts are geologically meaningful and provide temporal constraints on the geologic history of the Wrangellia terrane. Three of the reset $^{40}Ar/^{39}Ar$ ages (191, 181, and 161 Ma) of Karmutsen basalts from Vancouver Island are within the age range of Bonanza arc intrusions and volcanic sequences (197–167 Ma) that intrude and overlie the Karmtusen basalts on Vancouver

[6]Supplemental Methods File. This Microsoft Word file summarizes the analytical methods used for $^{40}Ar/^{39}Ar$ analyses. If you are viewing the PDF of this paper or reading it offline, please visit http://dx.doi.org/10.1130/GES00212.S6 or the full-text article on www.gsapubs.org to view the Supplemental Methods File.

[7]Supplemental Data File 3. Geochemistry for $^{40}Ar/^{39}Ar$ samples. This Microsoft Excel file contains the analytical data for whole-rock analyses for the 19 samples dated by the $^{40}Ar/^{39}Ar$ dating method. Analyses were performed by ActLabs and the analytical methods are summarized in Greene et al. (2009b). Additional information in this table includes: UTM coordinates, geographic location, lithology, mineral proportion, and texture. If you are viewing the PDF of this paper or reading it offline, please visit http://dx.doi.org/10.1130/GES00212.S7 or the full-text article on www.gsapubs.org to view Supplemental Data File 3.

[8]Supplemental Data File 4. $^{40}Ar/^{39}Ar$ analytical data. This Microsoft Excel file contains the analytical data for the $^{40}Ar/^{39}Ar$ dating method for the 20 mineral separates analyzed at the Noble Gas Laboratory in the Pacific Centre for Isotopic and Geochemical Research at University of British Columbia. Age spectra and isochron diagrams for each of the samples are shown along with all the analytical data from incremental step-heating. The analytical methods are summarized in the Supplemental Methods File. Where multiple analyses of a single sample were made, all the results for each sample are included in a single worksheet in this workbook. If you are viewing the PDF of this paper or reading it offline, please visit http://dx.doi.org/10.1130/GES00212.S8 or the full-text article on www.gsapubs.org to view Supplemental Data File 4.

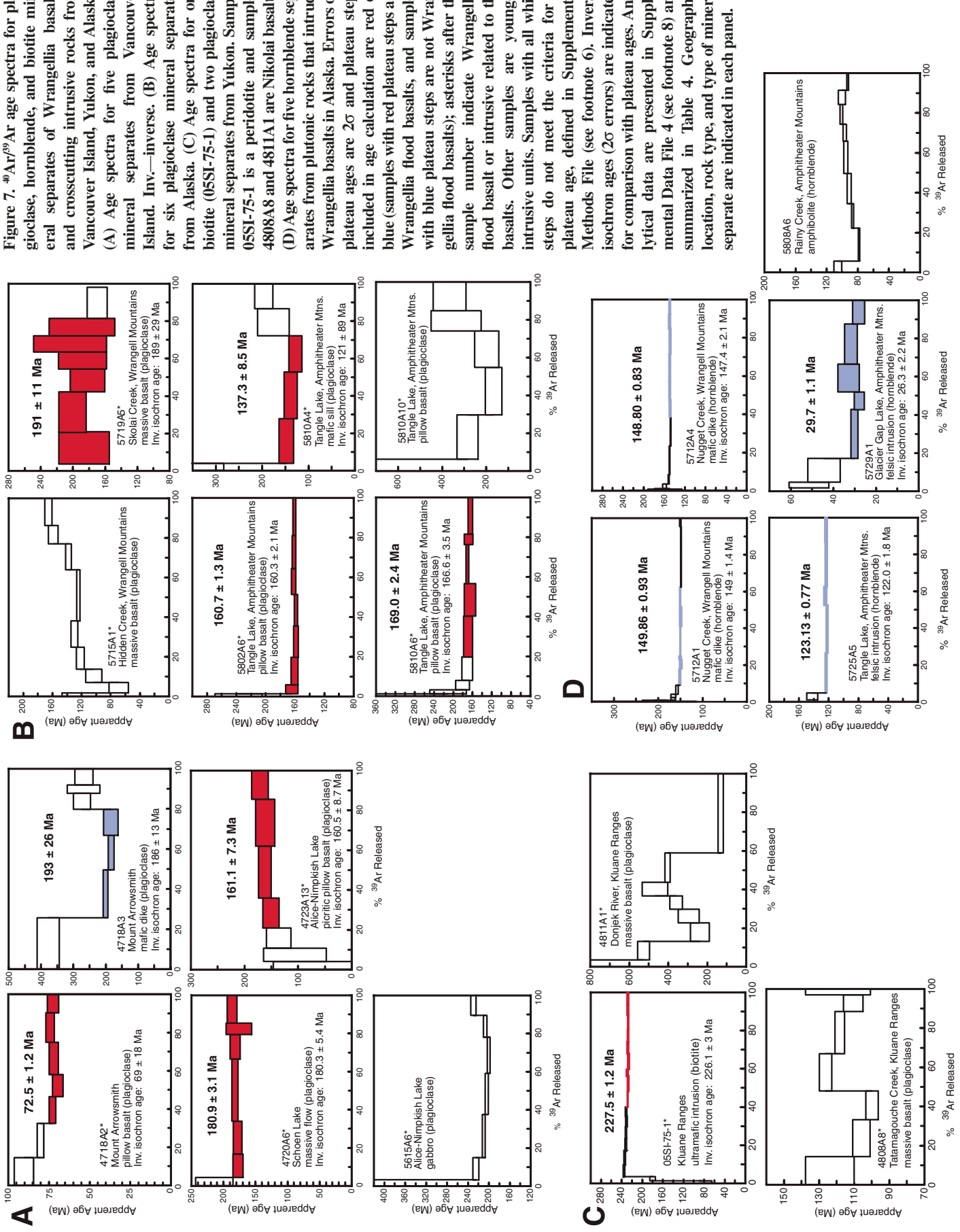

Figure 7. $^{40}Ar/^{39}Ar$ age spectra for plagioclase, hornblende, and biotite mineral separates of Wrangellia basalts and crosscutting intrusive rocks from Vancouver Island, Yukon, and Alaska. (A) Age spectra for five plagioclase mineral separates from Vancouver Island. Inv.—inverse. (B) Age spectra for six plagioclase mineral separates from Alaska. (C) Age spectra for one biotite (05SI-75-1) and two plagioclase mineral separates from Yukon. Sample 05SI-75-1 is a peridotite and samples 4808A8 and 4811A1 are Nikolai basalts. (D) Age spectra for five hornblende separates from plutonic rocks that intrude Wrangellia basalts in Alaska. Errors on plateau ages are 2σ and plateau steps included in age calculation are red or blue (samples with red plateau steps are Wrangellia flood basalts, and samples with blue plateau steps are not Wrangellia flood basalts); asterisks after the sample number indicate Wrangellia flood basalt or intrusive related to the basalts. Other samples are younger intrusive units. Samples with all white steps do not meet the criteria for a plateau age, defined in Supplemental Methods File (see footnote 6). Inverse isochron ages (2σ errors) are indicated for comparison with plateau ages. Analytical data are presented in Supplemental Data File 4 (see footnote 8) and summarized in Table 4. Geographic location, rock type, and type of mineral separate are indicated in each panel.

TABLE 4. $^{40}AR/^{39}AR$ DATING RESULTS FOR WRANGELLIA FLOOD BASALTS AND INTRUSIONS FROM THE WRANGELLIA TERRANE

Sample[†]	Mineral[§]	Integrated age (Ma)	Plateau age (Ma)[#]	Plateau information**	Inverse isochron (ages in Ma)[††]	Note
Vancouver Island		(2σ)	(2σ)			
4718A2*	Plag	76.31 ± 1.32	72.5 ± 1.2	5 steps 67.6% of ^{39}Ar released MSWD = 1.3	69 ±18 $(^{40}Ar/^{36}Ar)_i$ = 307 ± 65 MSWD = 1.14, n = 5	tholeiitic, pillowed flow
4718A3	Plag (1)	255.99 ± 10.86	193 ± 26	3 steps 54.3% of ^{39}Ar released MSWD = 5.1	186 ± 13 $(^{40}Ar/^{36}Ar)_i$ = 322.4 ± 9.6 MSWD = 2.6, n = 7	mafic dike
4718A3	Plag (2)	224.51 ± 10.33	NP		177.1 ± 3.1 $(^{40}Ar/^{36}Ar)_i$ = 327.5 ± 6.2 MSWD = 1.02, n = 6	last step: 231 ± 13 Ma
4718A3	Plag (C)	255.99 ± 10.86	NP		177.6 ± 3.0 $(^{40}Ar/^{36}Ar)_i$ = 325.3 ± 4.5 MSWD = 1.4, n = 9	combined high-T run #1, all run #2 inverse isochron
4720A6*	Plag	182.31 ± 3.20	180.9 ± 3.1	6 steps 95.6% of ^{39}Ar released MSWD = 0.93	180.3±5.4 $(^{40}Ar/^{36}Ar)_i$ = 307 ± 16 MSWD = 0.39, n = 7	tholeiitic, massive flow
4723A13*	Plag	150.24 ± 8.50	161.1 ± 7.3	4 steps 79.1% of ^{39}Ar released MSWD = 1.3	160.5 ± 8.7 $(^{40}Ar/^{36}Ar)_i$ = 280 ± 15 MSWD = 1.5, n = 7	slightly upstepping plateau, picritc pillow lava
5615A6*	Plag	220.98 ± 2.15	NP		NI	coarse-grained gabbroic rock
Yukon						
05SI-75-1*	Biotite	226.08 ± 0.53	227.5 ± 1.2	9 steps 60.1% of ^{39}Ar released MSWD = 1.6	226.1 ± 3 $(^{40}Ar/^{36}Ar)_i$ = 462 ± 380 MSWD = 1.7, n = 9	9 steps in plateau, peridotite
4808A8*	Plag	114.88 ± 2.60	NP		NI	high-Ti massive flow
4811A1*	Plag	361.37 ± 11.01	NP		NI	low-Ti massive flow
Wrangell Mountains						
5712A1	Plag	144.23 ± 1.08	145.6 ± 1.2	6 steps 84.6% of ^{39}Ar released MSWD = 0.91	146.5 ± 2.1 $(^{40}Ar/^{36}Ar)_i$ = 267 ± 48 MSWD = 0.72, n = 6	hbl-phyric hypabyssal rock
5712A1	Hbl	150.71 ± 0.53	149.86 ± 0.93	6 steps 53.5% ^{39}Ar released MSWD = 0.56	149.0 ± 1.4 $(^{40}Ar/^{36}Ar)_i$ = 359 ± 23 MSWD = 1.3, n = 9	hbl-phyric mafic intrusive rock
5712A4	Hbl	152.51 ± 0.63	148.80 ± 0.83	6 steps 61.4% of ^{39}Ar released MSWD = 0.67	147.4 ± 2.1 $(^{40}Ar/^{36}Ar)_i$ = 378 ± 96 MSWD = 2.9, n = 12	hbl-phyric mafic intrusive rock
5715A1*	Plag	131.21 ± 1.92	NP		NI	high-Ti massive flow
5719A5*	Plag	187.20 ± 10.44	191 ± 11	6 steps 82.4% of ^{39}Ar released MSWD = 0.48	189 ± 29 $(^{40}Ar/^{36}Ar)_i$ = 296 ± 21 MSWD = 0.16, n = 6	high-Ti massive flow
Alaska Range						
5725A5	Hbl	124.38 ± 0.69	123.13 ± 0.77	6 steps 95.2% of ^{39}Ar released MSWD = 1.5	122.0 ± 1.8 $(^{40}Ar/^{36}Ar)_i$ = 334 ± 18 MSWD = 0.51, n = 9	hbl-phyric felsic intrusive rock
5729A1	Hbl	37.59 ± 2.41	29.7 ± 1.1	5 steps 82.8% ^{39}Ar released MSWD = 1.9	26.3 ± 2.2 $(^{40}Ar/^{36}Ar)^i$ = 362 ± 20 MSWD = 0.46, n = 8	U-Pb zircon age[§§] 31.2 ± 0.2 Ma, hbl-phyric felsic intrusive rock
5802A6*	Plag	161.86 ± 1.31	160.7 ± 1.3	7 steps 98.6% of ^{39}Ar released MSWD = 1.13	160.3 ± 2.1 $(^{40}Ar/^{36}Ar)^i$ = 299 ± 16 MSWD = 0.88, n = 7	low-Ti sill
5808A6	Hbl (1)	92.77 ± 0.88	NP		NI	low-Ti dike, Rainy Creek
5808A6	Hbl (2)	87.14 ± 0.6	NP		NI	low-Ti dike, Rainy Creek
5810A4*	Plag	160.57 ± 8.64	137.3 ± 8.5	3 steps 68.3% of ^{39}Ar released MSWD = 1.7	121 ± 89 $(^{40}Ar/^{36}Ar)_i$ = 379 ± 470 MSWD = 0.17, n = 3	integrated age is preferred, low-Ti sill
5810A6*	Plag	180.30 ± 3.65	169.0 ± 2.4	5 steps 80.3% of ^{39}Ar released MSWD = 1.3	166.6 ± 3.5 $(^{40}Ar/^{36}Ar)_i$ = 321 ± 21 MSWD = 0.80, n = 8	low-Ti pillow basalt
5810A10*	Plag	325.39 ± 26.68	NP		NI	high-Ti pillow basalt

*Wrangellia flood basalt or intrusive equivalent, based on field relations, petrography, and geochemistry.

[†]Sample number: last digit year, month, day, initial, sample, except sample 05SI-75-1.

[§]Mineral separate and run number in parentheses, or (C) for combined result of multiple runs. Mineral abbreviations: hbl, hornblende; plag, plagioclase.

[#]Plateau age is preferred age, error reported for ± 2σ. NP—no plateau.

**Number of steps used for calculating age. Criteria for plateau age are described in the analytical methods in the Supplemental Methods File.

[††]Inverse isochron ($^{36}Ar/^{40}Ar$ vs. $^{39}Ar/^{40}Ar$) age, initial $^{40}Ar/^{36}Ar$ ratio, and MSWD. n—number of points included in isochron. MSWD—mean sum of the weighted deviates, which is a measure of the scatter compared to that which is expected from analytical uncertainties.

[§§]Unpublished data (A. Greene, 2009). NI—no isochron. See Supplemental Data File 3 (see footnote 7) for petrographic and geochemical data for all samples, and coordinates for sample locations. Supplemental Data File 4 (see footnote 8) presents the complete analytical results for $^{40}Ar/^{39}Ar$ analyses as an Excel workbook.

Island (Table 4; Nixon and Orr, 2007). The three reset ages of Nikolai basalts from the Amphitheater Mountains (169, 161, and 161 Ma) are similar to ages of felsic plutonic rocks of the Early to Middle Jurassic Talkeetna arc, in close proximity (<30 km) to the south (168–150 Ma; Rioux et al., 2007). In the Amphitheater and Talkeetna Mountains, Schmidt et al. (2003a) reported that reset plagioclase $^{40}Ar/^{39}Ar$ ages (174–152 Ma) for eight Nikolai basalts and gabbroic rocks are similar to the crystallization ages for these felsic plutonic rocks, which are assigned to the Peninsular terrane. A K-Ar isochron age of 112 ± 11 Ma was determined from seven Nikolai basalts in the Wrangell Mountains, indicating resetting of K-Ar systematics during tectonism related to northward transport of Wrangellia (MacKevett, 1978; Plafker et al., 1989). The hornblende $^{40}Ar/^{39}Ar$ ages are coincident with regional magmatic events reported from other studies in the areas in which these samples were collected. Two Late Jurassic ages of 148.8 ± 0.83 and 149.9 ± 0.93 Ma from mafic dikes in the Wrangell Mountains correspond with ages of Late Jurassic plutons of the Chitina arc (140–160 Ma; most ages between 145 and 150 Ma), ages that are synchronous with a major regional orogeny related to subduction (Grantz et al., 1966; MacKevett, 1978; Hudson, 1983; Dodds and Campbell, 1988; Plafker et al., 1989; Roeske et al., 2003).

In summary, the ages of Wrangellia flood basalts and intrusive rocks with associated analytical errors that are <±10 Myr (n = 9) are in the range from 222 to 233 Ma (Fig. 8 inset; Tables 3 and 4). The three U-Pb ages from mafic sills from Vancouver Island are within error of the four $^{40}Ar/^{39}Ar$ ages of basalts from Alaska that meet this precision criterion, as well as the $^{40}Ar/^{39}Ar$ plateau age of 227.5 ± 1.2 Ma given by biotite from a peridotite in this study. The slightly older age of 232.2 ± 1 Ma for a gabbro from Yukon (Mortensen and Hulbert, 1991) is the only age that is outside the range for the Vancouver Island samples, thus this gabbroic sill may represent an earlier phase of magmatism. The relatively narrow range of ages for Wrangellia flood basalts and associated intrusive rocks indicates that the duration of the majority of the magmatic activity was likely <5 Myr, occurring between ca. 230 and 225 Ma.

Paleontological Age Constraints

Fossils in sedimentary strata directly underlying and overlying the Wrangellia flood basalts also provide constraints on the age and duration of volcanism. MacKevett et al. (1964) reported that shale directly beneath Nikolai basalts on Golden Horn Peak in the Wrangell Mountains contained abundant Middle Triassic index fossils identified as *Daonella frami* Kittl. In 1971, a mineral exploration party discovered a sedimentary layer (<2 m thick) of fissile black shale between sills of Karmutsen basalts on Mount Schoen on Vancouver Island that contained imprints of *Daonella tyrolensis* (Carlisle, 1972). As part of the present study, samples of *Daonella* were collected from Golden Horn Peak in Alaska and on Mount Schoen on Vancouver Island. The *Daonella* specimens from both localities appear to have similar forms and are closely related to *Daonella frami* (C.A. McRoberts, 2006, personal commun.). The *Daonella* specimens appear older than Upper Ladinian forms, and are likely of middle Ladinian age (Poseidon Zone, ca. 235–232 Ma; C.A. McRoberts, 2006, personal commun.). Recovery of the conodont *Neospathodus* from these *Daonella* beds on Vancouver Island agrees with this age.

Magnetostratigraphic Age Constraints

Magnetic reversals were common throughout the Late Triassic; however, only a single magnetic polarity reversal is preserved in the Wrangellia flood basalts (Hillhouse, 1977). Magnetostratigraphy in the Newark rift basin of eastern North America has provided a high-resolution geomagnetic polarity time scale that reflects nearly idealized geomagnetic field reversal behavior in the Late Triassic (Kent and Olsen, 1999). A total of 59 polarity reversals occurred between 233 and 202 Ma; the mean duration of polarity intervals is estimated to be 0.53 Myr; the longest polarity interval is ~2 Myr and the shortest polarity interval is ~0.02 Myr (Kent and Olsen, 1999). All of the recorded polarity intervals between 225 and 230 Ma were at least ~0.5 Myr in duration. Based on this, the Wrangellia basalts likely erupted within a period of only 2 Myr and possibly in a considerably shorter time span.

DISCUSSION

Comparison of Northern and Southern Wrangellia

The stratigraphy and age of different areas of the Wrangellia oceanic plateau provide constraints on the construction of the volcanic stratigraphy, the paleoenvironments existing at the time of eruption, and the duration of volcanism. To aid in the following discussion, a summary of observed and previously reported field relationships of Wrangellia flood basalts, and the prevolcanic and postvolcanic rock record, is presented in Table 5, and a compilation of ages and biostratigraphy for Paleozoic–Triassic rocks of Wrangellia is presented in Figure 8 and Supplemental Data File 5[9]. We establish the similarities and differences in the stratigraphy of Northern and Southern Wrangellia and use them in subsequent sections to interpret the eruption environments and accumulation subsidence histories of different parts of this vast accreted oceanic plateau.

The basement of Wrangellia has different age strata in Alaska and Yukon than on Vancouver Island (Fig. 8, Supplemental Data Files 6[10] and

[9]Supplementary Data File 5. Wrangellia ages and biostratigraphy. This Microsoft Excel file contains three worksheets. (1) The Age worksheet contains ~750 isotopic ages for units assigned to Wrangellia. Most of this data was extracted from the CordAge 2004 database and was supplemented by ~50 ages not in the CordAge database, mostly from Alaska. Samples of the Coast and Insular Belts are included, based on their location, and caution should be used in deciding whether samples are actually located within Wrangellia. CordAge 2004 (a database of isotopic age determinations for rock units from the Canadian Cordillera) is an MS-Access based database, consisting of the merged datasets of the publically available products BCAge 2004A-1 (released October 2004; Breitsprecher and Mortensen (2004a)) and YukonAge 2004 (released July, 2004; Breitsprecher and Mortensen (2004b)). The compilation contains all reported non-proprietary isotopic age determinations for bedrock units from British Columbia and Yukon Territory, respectively: 9321 age determinations from 5997 rock samples, summarizing 778 published articles, theses, reports or unpublished sources. Katrin Breitsprecher offered assistance with extracting this information. The user is referred to Breitsprecher and Mortensen (2004a, 2004b) for information about the rating system of ages (**Rel_rating** column; column H) and other details. The database should not be cited as the source of the age. Age determinations should be cited to the original source, which is provided in each record of the database. (2) The Age_refs worksheet contains the information of the references for the age compilation listed in the Age worksheet (described above). The **ref no** column (column A) in the Age_refs worksheet refers to the **Ref No** column (column L) in the Age worksheet. (3) The Biostratigraphy worksheet is a compilation of 75 fossil age determinations from published literature related to Wrangellia. The full reference where each determination is published is included in column B and the region is shown in column E. All of the age ranges are plotted in Figure 8 according to the region indicated in column E. The low and high ages for each age range use the age boundaries for epochs and stages from Gradstein et al. (2004). Age boundaries for the Triassic are from Ogg (2004) and revised based on Furin et al. (2006). If you are viewing the PDF of this paper or reading it offline, please visit http://dx.doi.org/10.1130/GES00212.S9 or the full-text article on www.gsapubs.org to view Supplemental Data File 5.

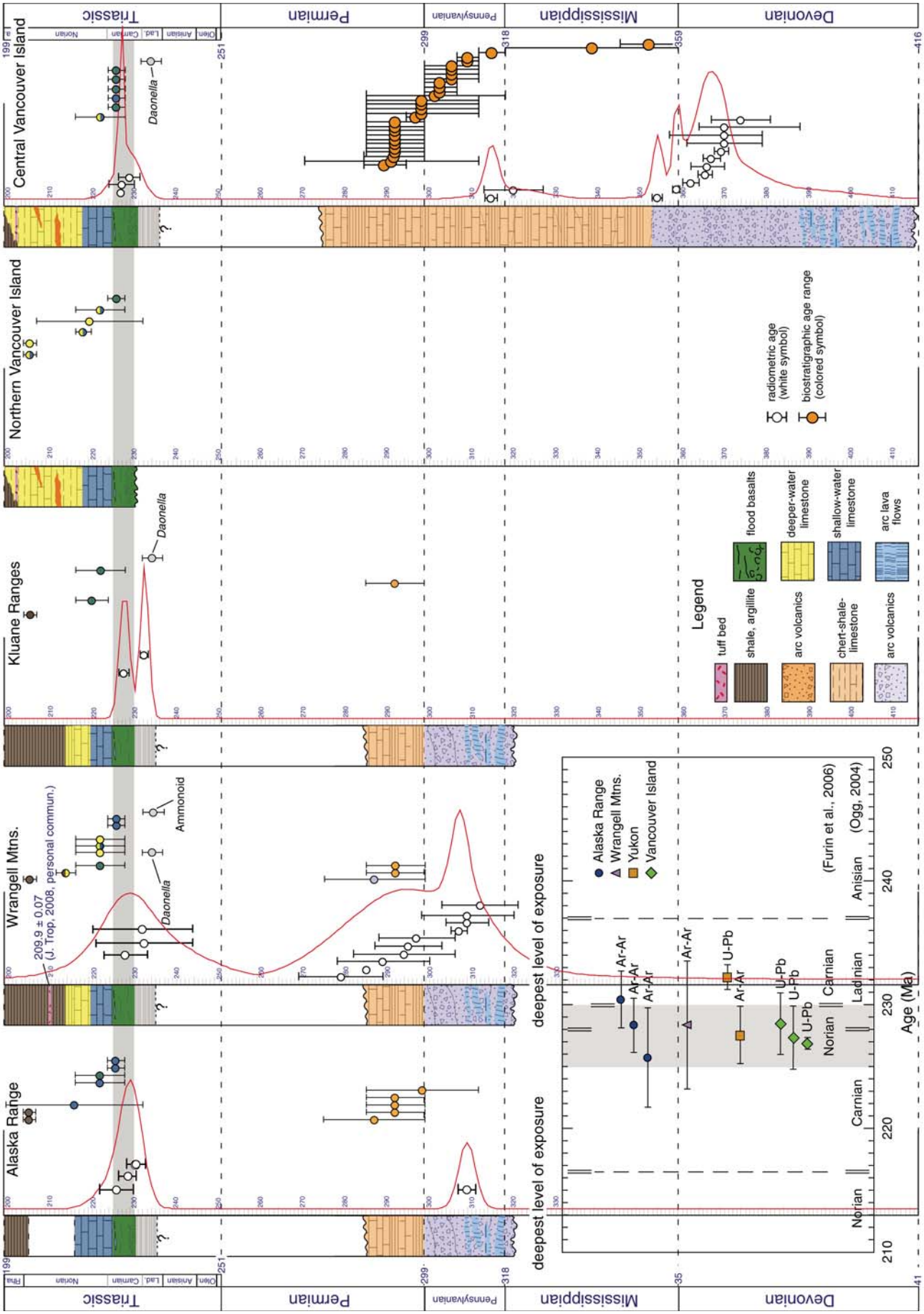

Figure 8. Summary of ages and biostratigraphy in five areas of Wrangellia. Radiometric ages are white circles. Fossil ages are colored according to the formation they are found in the stratigraphic column. Circles that are multicolored green and blue indicate fossils from interflow sedimentary lenses, and other multicolored circles indicate fossils found near the contact between two formations. Information for age data and biostratigraphy are presented in Supplemental Data File 5 (see footnote 9). Age probability density distribution plots for each area are calculated from the plotted ages using AgeDisplay (Sircombe, 2004). The ages for the period boundaries are from Gradstein et al. (2004). Ages for epoch boundaries of the Triassic are adjusted using Furin et al. (2006). Inset is a summary diagram showing $^{40}Ar/^{39}Ar$ and U-Pb ages of Wrangellia flood basalts and plutonic rocks with analytical uncertainty <10 Myr total. The results are shown from north (top) to south (bottom) and are distinguished by region. Analytical details are presented in Tables 3 and 4. Two schemes are shown for the boundaries of part of the Triassic, from Furin et al. (2006) and Ogg (2004). Errors are 2σ. Gray fields in the inset and main diagram indicate 230–225 Ma.

7[11]). The basement of Wrangellia was originally defined as a Pennsylvanian–Permian volcanic arc sequence that may have been deposited on oceanic crust (Jones et al., 1977), and this has been maintained by numerous authors (Smith and MacKevett, 1970; MacKevett, 1978; Coney et al., 1980; Monger et al., 1982; Saleeby, 1983; Beard and Barker, 1989). However, whereas Pennsylvanian–Permian volcanic arcs are preserved in Alaska (Smith and MacKevett, 1970; MacKevett, 1978; Beard and Barker, 1989), older Paleozoic rocks make up much of Vancouver Island (Muller, 1977; Brandon et al., 1986), and there is no significant arc volcanism in the Pennsylvanian–Permian of Vancouver Island (Fig. 8; Yole, 1969; Massey and Friday, 1988; Yorath et al., 1999). The Paleozoic volcanic sequences on Vancouver Island are considerably older (ca. 380–355 Ma) than dated volcanic sequences in Alaska (ca. 312–280 Ma, mostly from the Wrangell Mountains; see Fig. 8 and references therein). Paleozoic limestone beneath Wrangellia basalts in Alaska contains Early Permian bryozoans, brachiopods, foraminifera, and corals (Smith and MacKevett, 1970). On Vancouver Island, conodonts in the Buttle Lake Group indicate Mississippian–Permian ages (Orchard *fide* Brandon et al., 1986; Orchard, 1986; Fig. 8; Supplemental Data File 5 [see footnote 9]).

The volcanic stratigraphy on Vancouver Island consists of a tripartite succession of submarine flows (50%–60% of total thickness), volcaniclastics, and subaerial flows, whereas volcanic stratigraphy in Alaska and Yukon is predominantly subaerial flows (>90%; Table 5; Greene et al., 2008, 2009a, 2009b). In areas of central Vancouver Island, the stratigraphically lowest pillow basalts were emplaced on unconsolidated fine-grained sediments, and mafic sills intrude marine strata with *Daonella* beds. In other areas of central and southern Vancouver Island, basal basalt flows overlie Permian limestone and sills intrude this limestone (Fig. 6). The submarine section on Vancouver Island (~3000 m) is substantially thicker than in the Alaska Range (<800 m). In the Alaska Range, the stratigraphically lowest submarine flows were emplaced on nonfossiliferous black shale. In the Wrangell Mountains, a basal flow conglomerate directly overlies shale with *Daonella* beds and contains erosional remnants from the underlying Paleozoic units. Laterally discontinuous zones of conglomerate along the base of the Nikolai Formation in Yukon have been interpreted as syntectonic deposits and flows related to the formation of grabens (Israel et al., 2006). The flood basalts in Northern Wrangellia are low-Ti basalts (<400 m) overlain by high-Ti basalts, whereas almost all of the basalt stratigraphy in Southern Wrangellia is high-Ti basalt and includes an area 30 km in diameter with abundant picritic pillow basalts (Greene et al., 2008, 2009a, 2009b).

The overlying limestone and interflow sedimentary lenses in Northern and Southern Wrangellia are lithologically similar and have a similar range of fossil ages (Table 5; Fig. 8). In Southern Wrangellia, interflow sedimentary lenses are common in the upper parts of the Karmutsen Formation and the overlying limestone contains late Carnian–Norian fossils. Within upper Nikolai Formation stratigraphy in Northern Wrangellia, interflow sedimentary lenses occur in southwest Yukon and the Clearwater Mountains, and Nikolai basalts are overlain by limestone with age-diagnostic late Carnian–early Norian fossils. Sedimentary strata extend up through the Triassic-Jurassic boundary in Northern and Southern Wrangellia. The interflow limestone lenses and overlying sedimentary rocks are important time and depth markers for estimating the subsidence and mantle thermal history of Wrangellia (see following discussion). Based on the similar age, high effusion rate, tectonic history, and trace element and isotopic geochemistry of Wrangellia basalts (Greene et al., 2008, 2009a, 2009b), the flood basalts of Northern and Southern Wrangellia are interpreted to have formed from the same plume-related magmatic event.

Eruption Environment for Wrangellia Flood Basalts

Northern Wrangellia

The Nikolai basalts in Alaska were emplaced as effusive eruptions in a shallow marine and subaerial environment (Fig. 9). Sedimentary rocks directly beneath the flood basalts in the Alaska Range are mostly siliceous argillites, carbonaceous black shales, and mudstones; the upper part of the 200–250 m sequence has a higher proportion of black carbonaceous shale and carbonate (Blodgett, 2002). In this area, Blodgett (2002) interpreted the total absence of fossils and biogenic sedimentary structures (trace fossils), and the even, parallel laminations (indicating lack of bioturbation), as indicative of deposition in a starved, anoxic shallow submarine environment. The higher proportion of black carbonaceous shale and calcareous component for sediments higher in the sequence may indicate a shallower depositional environment for the younger sediments than for the older sediments, possibly due to uplift prior to eruption (Blodgett, 2002). The pillow basalts in the Alaska Range (~500 m) are highly vesicular, consistent with eruption in shallow water (Jones, 1969; Kokelaar, 1986). Volcaniclastic

[10]Supplemental Data File 6. Previous research on Wrangellia. This Microsoft Word file is a summary of previous research on parts of the Wrangellia terrane in Alaska, Yukon, and British Columbia that includes many references. These references and others are listed in Supplemental Data Files 1 and 2. If you are viewing the PDF of this paper or reading it offline, please visit http://dx.doi.org/10.1130/GES00212.S10 or the full-text article on www.gsapubs.org to view Supplemental Data File 6.

[11]Supplemental Data File 7. Stratigraphy of Wrangellia. This Microsoft Word file presents a detailed description of the stratigraphy of Wrangellia. See the Supplementary Figure File for nine figures that accompany this summary of the stratigraphy. If you are viewing the PDF of this paper or reading it offline, please visit http://dx.doi.org/10.1130/GES00212.S11 or the full-text article on www.gsapubs.org to view Supplemental Data File 7.

TABLE 5. COMPARISON OF GEOLOGY AND AGES OF NORTHERN AND SOUTHERN WRANGELLIA

Northern Wrangellia	Southern Wrangellia
Rocks overlying the Nikolai Formation	Rocks overlying the Karmutsen Formation
Clastic sedimentary sequences above Nikolai span Triassic-Jurassic boundary	Clastic sedimentary sequences above Karmutsen span Triassic-Jurassic boundary
Late Carnian to early Norian fossils in overlying limestone	Late Carnian to Early Norian fossils in overlying limestone
Overlying limestone grades upward from shallow water to deeper water facies	Overlying limestone grades upward from shallow water to deeper water facies
Nikolai basalts interbedded with limestone and argillite (Yukon)	Limestone and sedimentary rocks of the Kunga and Maude Groups on Haida Gwaii
Limestone is commonly brecciated near the base	Kunga Formation contains identical fossils to Quatsino limestone
	Karmutsen basalt, or younger basalt, locally intrudes the Quatsino limestone
Thin layer of siltstone in several locations along Nikolai-Chitistone contact	Mostly micritic limestone directly overlying the basalts
Occurrences of regolith between the top of the Nikolai and the base of the Chitistone	Thin (<25 cm) layer of siltstone immediately overlying basalt in several locations
	Little evidence of erosion between Karmutsen and Quatsino limestone
Nikolai Formation	Karmutsen Formation
4 U-Pb and Ar-Ar ages (uncertainty <±10 Myr) of 225–230 Ma (with one Yukon outlier)	3 U-Pb ages (uncertainty <±10 Myr) of 226–228 Ma
Late Carnian to early Norian fossils in limestone lenses in Yukon	Regolith above uppermost flow
Trachytic-textured plagioclase-rich flows near top of Nikolai in Wrangell Mtns	Intraflow limestone and/or clastic lenses near top formed in shallow submarine areas
Predominantly massive subaerial flows	Late Carnian to early Norian fossils in sedimentary lenses within upper Karmutsen
	Plagioclase-megacrystic flows near the top of the basalt succession
Alaska Range (Amphitheater and Clearwater Mountains)	*Vancouver Island*
~7% of lowest part of stratigraphy is pillow basalt (<500 m), and ~3000 m subaerial flows	Flood basalts form emergent basalt sequence
Pillows tend to have mostly small diameter (<1 m)	Subaerial stage—subaerial flows (>2500 m on CVI, <1500 m on NVI)
Pillows have abundant vesicles (20–30 vol%) indicating eruption in shallow water (<800 m)	Shallower water stage—pillow breccia and/or hyaloclastite (400–1500 m on NVI)
Vesicles in pillows are spherical (<1 mm) and evenly distributed throughout pillows	Deeper water stage—pillowed and massive basalt flows (>2500 m)
Megapillows rare in Alaska	
Minor amounts of breccia and tuff within submarine section	Pillow basalts erupted in deeper marine setting than in Northern Wrangellia
Interbedded limestone and/or clastic near top of Nikolai in Clearwater Mtns and in Yukon	Most pillows are commonly large diameter (>1 m)
Thick sediment-sill complex	Pillows are more commonly nonvesicular or have radially oriented pipe vesicles
Large area of complementary plutonic rocks represent feeder system for flood basalts	Megapillows (>4 m) within pillowed flows on VI
No sheeted dike complexes, sill-dominated feeder system	Volcaniclastic rocks formed primarily via cooling-contraction granulation
Rare dikes	Volcaniclastics mostly between pillow basalt and subaerial flow units
Black shale within sediment-sill complex, nonfossiliferous (starved, anoxic environment)	Peperites in submarine section
Picritic pillow lava near base of submarine section in Clearwater Mtns	Subaerial flow unit is conformable with the underlying hyaloclastite unit
Pillow basalt engulfs fine-grained sediment in lowermost pillowed flows	
Picritic tuff found outside the main area of flood basalts (possibly related to Nikolai basalts)	

(*continued*)

TABLE 5. COMPARISON OF GEOLOGY AND AGES OF NORTHERN AND SOUTHERN WRANGELLIA (continued)

Northern Wrangellia	Southern Wrangellia
Wrangell Mountains and Kluane Ranges	Rare occurrences of interflow sediments, aside from lenses between upper flows
Occurrences of regolith between top of Nikolai and overlying Chitistone limestone	Columnar jointing is rare, irregular jointing in massive submarine flows
Rare thin argillite (<10 cm) on top of uppermost flow	Rare dikes, no sheeted dike complexes
Intraflow limestone lenses (1–30 m thick) near top formed in shallow submarine areas	Thick sediment-sill complexes where base is exposed on VI
Plagioclase-megacrystic flows near the top of the basalt succession	Increase in vesicularity and proportion of volcaniclastics upwards in submarine unit
Almost no pillow basalt in basalt stratigraphy (only in lowermost ~70 m)	Pahoehoe structures (e.g., ropy festoons) within flows and just below Quatsino limestone
Pillow breccia and polymictic flow-conglomerate in lowermost ~70 m	Piciritc pillow lavas in upper part of the submarine section on NVI
Basal flow-congolmerate directly overlies argillite with fissile *Daonella* beds	Marine fossils in pillow breccia, Buttle Lake area
Abundant rounded clasts derived from underlying Paleozoic formations	Pillow basalt engulfs fine-grained sediment in lowermost pillowed flows
Larger pendants (>100 m long) of Paleozoic rocks in lowermost flows	Submarine basalts form volumetrically minor part of the subaerial stratigraphy
	No clear indication of uplift prior to eruption on VI
~3500 m of subaerial sheet flows; columnar jointing is rare	
	Queen Charlotte Islands (Haida Gwaii)
Very rare occurrences of interflow sediments, other than lenses in upper part	One measured section (~4300 m): 95% submarine, pillow to fragmental ratio (8:2)
Quartz-pebble conglomerate in sediments beneath Nikolai in Talkeetna Mtns	Local tuffaceous crinoidal limestone lenses in lowermost flows
Rocks underlying the Nikolai Formation	Rocks underlying the Karmutsen Formation
Paleozoic arc sequences not exposed in Talkeetna Mtns beneath Nikolai	Permian chert, carbonate, and volcaniclastic rocks form deepest level of exposure
Wrangell Mountains and Kluane Ranges	
Evidence of erosional surface beneath Nikolai, rounded clasts from underlying sequences	*Daonella* imprints in shale within sediment-sill complex on Mount Schoen, VI
Rounded pebble- to cobble-size clasts indicate subaerial or shallow submarine reworking	*Daonella* imply dysoxic bottom waters typical of mud-dwellers
Indication of uplift prior to eruption in Wrangell Mountains	
Coarse-grained mafic intrusions intrude and deform underlying sedimentary sequences	Coarse-grained mafic rocks intrude and deform underlying sedimentary sequences
Daonella imprints in fissile shale underlying lowermost pillow breccia	Mafic sills intrude siliceous argillite, shale, chert, and limestone
Erosional unconformity between *Daonella* beds and underlying Paleozoic limestone	
Formation of laterally discontinuous grabens along base in Kluane Ranges	
Alaska Range (Amphitheater and Clearwater Mountains)	Paleozoic sequences mostly exposed in two anticlinoria on central and southern VI
Pre-Nikolai sediments grade upward from siliceous argillite to carbonaceous black shale	
Pre-Nikolai black shale deposited in starved, anoxic marine setting	Conodonts indicate Mississippian to Permian ages in the Buttle Lake Group
No bioturbation (parallel laminations) and no biogenic structures (trace fossils)	
Coarse-grained mafic rocks intrude and deform underlying sedimentary sequences	Paleozoic arc sequences underlying Karmutsen basalts with ages of 380–355 Ma
Limestone (with Early Permian fossils), chert, argillite underlying Nikolai basalts	Oldest known rocks on Vancouver Island are the Devonian Duck Lake Formation
Paleozoic arc sequences underlying Nikolai basalts with ages of 312–280 Ma	
No rocks dated older than Pennsylvanian in Wrangellia in Alaska	

Note: References not included in this table, see supplementary data files for references.VI—Vancouver Island; CVI—central Vancouver Island; NVI—northern Vancouver Island.

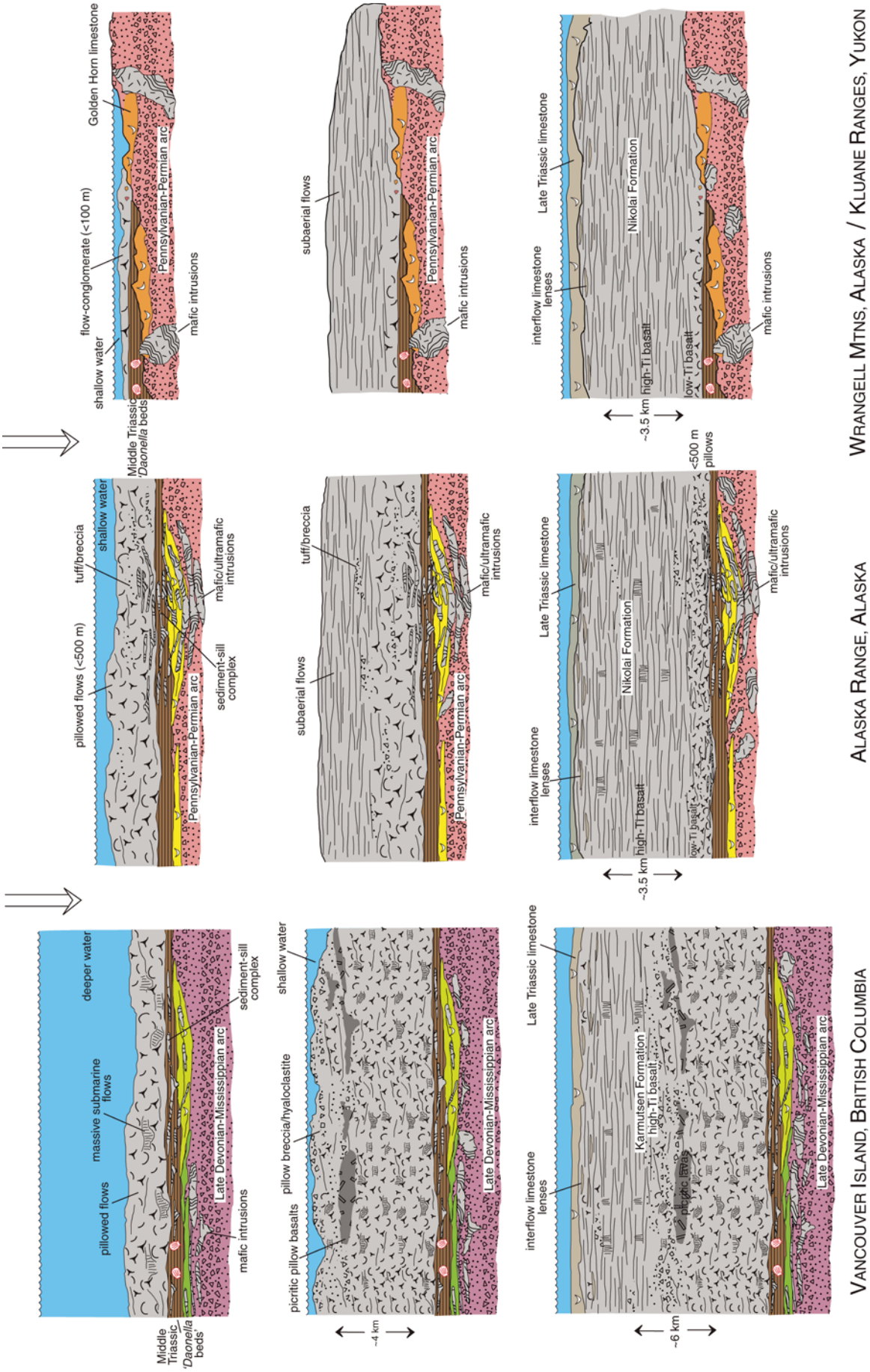

Figure 9. Interpretative diagrams showing the construction of the Wrangellia oceanic plateau. From top to bottom, the diagrams depict the eruption environment and growth of the volcanic stratigraphy for areas of Wrangellia flood basalts on Vancouver Island and in Alaska and Yukon. Prevolcanic and postvolcanic sedimentary sequences and underlying Paleozoic arc units are also shown. The emergent stage of the Karmutsen Formation on Vancouver Island is indicated by subaerial flows and is not shown in a separate diagram for space consideration. Most of the units in the sketches are labeled, so there is no accompanying legend. White arrows indicate downward progression of time sequence in diagrams. Volcanic activity in each of the areas initiated with submarine flows emplaced onto pelagic sediments and all of the flood basalts are overlain by Late Triassic limestone. See interpretation of eruption environments for further discussion. See Figure 8 for specific age and biostratigraphic information on units and Table 5 for detailed descriptions of field relationships.

flows intercalated with pillow basalt also indicate eruption in shallow water; this transition typically occurs in <200 m water depth for tholeiitic magmas (Kokelaar, 1986). The subaerial flows (>3000 m) were emplaced as inflated compound pahoehoe flow fields during prolonged, episodic eruptions similar to those in most continental flood basalts (e.g., Self et al., 1997). The flows erupted from a limited number of eruption sites that are rarely observed, except for a large sill-dominated eruptive center in the Amphitheater Mountains.

In the Wrangell Mountains and Yukon, the basal flow conglomerate and pillow breccia (<100 m thick) erupted in shallow water (<200 m; Fig. 9). Rounded clasts in the basal flow conglomerate indicate an area of relief near sea level in the Wrangell Mountains. Above the basal flow unit in the Wrangell Mountains are ~3500 m of subaerial sheet flows that lack features of submarine emplacement. The proportion of amygdules in the massive flows is variable, but generally high, similar to many continental flood basalts. In contrast, submarine sheet flows exposed in accreted portions of the Ontong Java Plateau in the Solomon Islands of the western Pacific Ocean rarely have vesicles (Petterson, 2004); pillowed and massive flows are preserved throughout the stratigraphy of the Ontong Java Plateau.

Southern Wrangellia

The tripartite Karmutsen stratigraphy on Vancouver Island formed as an emergent basalt sequence that passed through a deeper water, shallow water, and subaerial stage, similar in ways to those described in the formation of emergent seamounts (Fig. 9; Schmidt and Schmicke, 2000) and Hawaiian volcanoes (Garcia et al., 2007). Sills obscure relationships at the sediment-basalt interface at the base of the Karmutsen Formation, and there may have been sediments on top that are no longer preserved, but most of the fine-grained strata underlying the Karmutsen were deposited below storm wave base. Carlisle (1972) reported that pre-Karmutsen sediments show a progressive change from coarse bioclastic limestone to laminated and silicified shale, indicating a transition from an organic-rich, shallow-water environment to a starved, pelagic deeper water depositional environment prior to initiation of volcanism. *Daonella* fossils in fine black shale from near the top of this unit imply dysoxic bottom waters typical of mud dwellers that float on soupy sediments (Schatz, 2005).

The deeper water stage (>200 m water depth) of the Karmutsen Formation was dominated by effusive activity that formed pillowed and massive flows (Greene et al., 2009). The pillowed flows are interconnected tubes and lobes that contain large-diameter pillows (>2 m) and have low abundances of amygdules. The massive flows may represent some of the master tubes for delivery to distal parts of flow fields or locally increased effusive rates, due to topography, as evinced by concave basal contacts. The basalts increase in vesicularity, as does the proportion of volcaniclastics, upward in the submarine stratigraphy (Nixon et al., 2008).

The shallow-water stage of the Karmutsen preserves an increasing proportion of volcaniclastic units (pillow breccia and hyaloclastite) conformably overlying mostly close-packed pillows. The pillow breccias are commonly associated with pillowed flows and contain aquagene tuff (Carlisle, 1963) or redeposited hyaloclastite. The transition from close-packed pillowed flows to pillow breccia and hyaloclastite probably occurred in <500 m water depth; however, in certain areas on northern Vancouver Island the volcaniclastic unit is >1500 m thick (Nixon et al., 2008). Sedimentary structures (e.g., graded bedding, fluidization structures) are present locally and indicate resedimentation processes. Pyroclastic deposits containing lapilli tuff and volcanic bombs do not appear to be common (Carlisle, 1963). The volcaniclastic rocks likely formed primarily via cooling-contraction granulation, magma-water-steam interaction, autobrecciation, and mass wasting, rather than pyroclastic eruption.

The emergent subaerial stage is marked by the relative absence of volcaniclastic and pillowed flow units and dominance of massive amygdaloidal sheet flows. The sheet flows were emplaced as inflated compound pahoehoe flow fields atop an enormous oceanic plateau. There are isolated sections of submarine flood basalts (<200 m thick) within the uppermost subaerial Karmutsen stratigraphy (Surdam, 1967; Carlisle and Suzuki, 1974); these units form a volumetrically minor component of the subaerial stratigraphy. The intra-Karmtusen sedimentary lenses formed in isolated, low-lying areas in a predominantly subaerially exposed plateau (Carlisle and Suzuki, 1974).

There are similarities between the stratigraphy of Karmutsen basalts and the stratigraphy of the Hawaii Scientific Drilling Project core (HSDP2; Garcia et al., 2007). In both the Karmutsen basalts and HSDP2, predominantly pillowed flows in the lower parts of the submarine stratigraphy give way to increasing proportions of volcaniclastic units upsection, below the submarine-subaerial transition. Vesiculated pillows of the Karmutsen Formation on Northern Vancouver Island are more common near the top of the pillow unit and in the hyaloclastite unit. HSDP2 drill core shows an increase in vesicularity with decreasing depth in the submarine lava flows (Garcia et al., 2007). Intrusions are more common in the lower parts of the stratigraphy within both submarine sections and, although more difficult to identify, they appear to be less common within the subaerial sections. In contrast, flow morphologies and thicknesses are distinct in Karmutsen stratigraphy and Hawaiian volcanoes.

Accumulation and Subsidence of the Wrangellia Basalts

The geology, age, and biostratigraphy of Wrangellia can be used to estimate the rate of accumulation of Wrangellia basalts and the subsidence of the Wrangellia oceanic plateau. Carlisle and Suzuki (1974) originally estimated an accumulation rate for the Karmutsen basalts of 0.17–0.27 cm/yr over 2.5–3.5 Myr. This yielded a total erupted volume of basalt of 3.7–4.0 × 10^5 km^3 (they assumed an area 400 km × 150 km, roughly the size of Vancouver Island, or 60 × 10^3 km^2, and a stratigraphic thickness of 6 km) and a volumetric output rate of 0.10–0.16 km^3/yr (Carlisle and Suzuki, 1974). The area of exposure of Karmutsen basalts in this study was calculated using digital geology maps for exposures of the Karmutsen Formation on Vancouver Island and the Queen Charlotte Islands, and represents a minimum estimate of surface area. The estimated total erupted volume and volumetric output rate were calculated using a stratigraphic thickness of 6 km and duration of volcanism of 5 Myr. Our estimate of minimum volcanic output rate is ~0.03 km^3/yr and that of minimum total erupted volume of Karmutsen basalts is 1.4–1.5 × 10^5 km^3. Even using this very conservative estimate for the area of exposure and age, the volumetric output rate is comparable to recent estimates of long-term volumetric eruption rates for ocean islands such as Iceland (0.02–0.04 km^3/yr) and Hawaii (0.02–0.08 km^3/yr) (White et al., 2006).

Subsidence of the Karmutsen basalts during volcanism was recorded by the deposition of interflow sedimentary lenses between the upper flows during the waning stages of volcanism as low-lying areas of the plateau were submerged. The occurrence of interflow lenses indicates that by the end of Karmutsen flood volcanism most of the top of the basalt plateau had subsided and submerged below sea level. This implies that over the duration of subaerial volcanism, the rate of accumulation of basalt flows was comparable to the rate of subsidence. Carbonate deposition was preserved during the waning stage of volcanism, and there was no significant break after volcanism ceased. There are few signs of erosion between the Quatsino

limestone and Karmutsen Formation (in places only a <25 cm thick siltstone and/or sandstone layer is preserved), and interflow lenses have fossils identical to those of the lower part of the Quatsino limestone.

Postvolcanic subsidence of the Wrangellia oceanic plateau is recorded by hundreds of meters to >1000 m of Late Triassic marine sedimentary rocks overlying the basalt stratigraphy. The Quatsino limestone was deposited on top of the plateau as it began to submerge beneath sea level, and while volcanism waned. Deposition continued as the plateau became fully submerged and the sea transgressed over the entire plateau. Initially, intertidal to supratidal limestones were deposited in shallow-water, high-energy areas, some of the limestones reflecting quieter, subtidal conditions (Carlisle and Suzuki, 1974). Upsection, the Quatsino Formation reflects a slightly deeper water depositional environment and abruptly grades into the overlying Parson Bay Formation (Carlisle and Suzuki, 1974; Nixon and Orr, 2007).

In Alaska and Yukon, the carbonate rocks overlying the Nikolai basalts (>1000 m; Chitistone and Nizina limestones) preserve a record of the gradual submergence of the extensive Nikolai basalt platform. There are only rare occurrences of thin (<0.5 m) weathered zones or discontinuous, intervening clastic deposits at the top of ~3500 m of subaerial basalt flows in the Wrangell Mountains (Fig. 3; Armstrong et al., 1969). The absence of significant erosion or deposition of clastic sediment and the age of the Chitistone limestone (Fig. 8) indicate only a brief interval of nondeposition between the end of volcanism and carbonate deposition. Following volcanism, several cycles of shaley to argillaceous limestone were deposited in a high-energy, intertidal to supratidal (sahbka) environment, similar to the modern Persian Gulf, and form the lowest 100 m of the Chitistone limestone (Armstrong et al., 1969). Limey mudstone and wackestone with abundant disintegrated shelly material (~300 m thick) indicate a gradual transition to low-energy shallow-water deposition with intermittent high-energy shoaling deposition. The upper part of the Chitistone and overlying Nizina limestones reflect deeper water deposition on a drowned carbonate platform (Armstrong et al., 1969). Gray to black shale and chert of the overlying McCarthy Formation represent submergence of the carbonate platform below the carbonate compensation depth (Armstrong et al., 1969). A thin tuff bed in the lower part of the McCarthy Formation has been dated at 209.9 ± 0.07 Ma (J. Trop, 2006, personal commun.), and the Triassic-Jurassic boundary is preserved in the upper McCarthy Formation (Fig. 8). Between the end of basaltic volcanism and the end of the Triassic (~25 Myr), ~2000 m of shallow- to deep-water marine sediments accumulated on top of the Nikolai basalts. Neglecting sediment compaction, this indicates a minimum subsidence rate of ~80 m/Myr. This subsidence decreased substantially, to <20 m/Myr, in the Early Jurassic (Saltus et al., 2007). Initial subsidence rates of 50 m/Myr were also estimated by Richards et al. (1991) based on the thickness and age of carbonate rocks overlying the Nikolai Formation.

Several oceanic plateaus and ocean islands worldwide preserve evidence of rapid subsidence after their formation (Detrick et al., 1977), and mantle plume models predict subsidence following the formation of oceanic plateaus (e.g., Campbell and Griffiths, 1990). Subsidence may result from dispersion of the mantle buoyancy anomaly above a plume; decay of the thermal anomaly and cooling and contraction of the lithosphere; removal of magma from the plume source, causing deflation of the plume head; and/or depression of the surface from loading of volcanic and plutonic material on the lithosphere (e.g., Detrick et al., 1977; Campbell and Griffiths, 1990). Hawaiian volcanoes undergo rapid subsidence during their growth due to the response from loading of intrusive and extrusive magmas on the lithosphere (e.g., Moore and Clague, 1992). Pacific Cretaceous plateaus, such as Ontong Java, Manihiki, and Shatsky Rise, underwent significantly less subsidence than predicted by current models, with post–flood basalt subsidence comparable to that of normal ocean seafloor (Ito and Clift, 1998; Roberge et al., 2005). Drilling of the Kerguelen Plateau indicates that subaerial flows, perhaps originally 1–2 km above sea level, subsided below sea level and paleoenvironments of the overlying sediments changed from intertidal to pelagic (Coffin, 1992; Frey et al., 2000; Wallace, 2002). Subsidence estimates for the Northern Kerguelen Plateau (Ocean Drilling Program Leg 183, Site 1140) indicate that ~1700 m of subsidence occurred since eruption of the basalts at 34 Ma (~50 m/Myr; Wallace, 2002). The subsidence history of Wrangellia may be more fully reconstructed by future studies that estimate the depth of sedimentation and age from microfossils collected from sediments overlying the Karmutsen and Nikolai Formations. The well-preserved and accessible sedimentary strata overlying the accreted Wrangellia plateau has the potential to affect our understanding of the thermal history of oceanic plateaus from plume-controlled magmatic events that are not associated with mid-ocean ridge processes, such as several oceanic plateaus in the Pacific (e.g., Shatsky Rise; Sager, 2005).

IMPLICATIONS FOR THE ARCHITECTURE OF OCEANIC PLATEAUS

The architecture of the erupted products of oceanic plateaus provides one of the most direct ways of evaluating the largest magmatic events on Earth. Construction of oceanic plateaus has implications for the age and duration of magmatism, the association of plume- or plate-controlled processes, uplift and subsidence history related to large magmatic events, mantle melting processes and thermal evolution, and the effect of eruptions on the environment (e.g., Ito and Clift, 1998; Wignall, 2001; Sager, 2005; Saunders et al., 2007). The Wrangellia plateau provides an unmatched view of the preeruption, syneruption, and posteruption phases of the growth of plume-related oceanic plateaus on Earth. Here we compare Wrangellia to other oceanic plateaus, and to continental flood basalts and modern ocean island hotspots, to highlight the conditions and processes that control the formation of oceanic plateaus.

Based on the stratigraphic and temporal constraints outlined in this study, and the petrology and geochemistry of the Wrangellia basalts from Greene et al. (2008, 2009a, 2009b), the main factors that controlled the construction of the Wrangellia oceanic plateau include high effusion rates and the formation of extensive compound flow fields from low-viscosity, high-temperature tholeiitic basalts, sill-dominated feeder systems, low volatile content, protracted eruption (perhaps >10 yr for individual flow fields), limited repose time between flows (absence of weathering, erosion, sedimentation), submarine versus subaerial emplacement, and relative water depth (e.g., pillow basalt–volcaniclastic transition). Combined, these factors contributed to the production of 4–6 km of basalt stratigraphy with limited magnetic reversals, a lack of fossil remains in associated sediments, and minimal evidence of eruptive explosivity. In Table 6, the major features of the Wrangellia, Ontong Java, and Caribbean oceanic plateaus are compared. From this comparison, several commonalities are evident, including high effusive rates, sill-dominated feeder systems, largely submarine eruptions (but varying amounts of subaerial eruptions), presence of high-MgO lavas, absence of alkalic lavas during the main eruptive phase, and relatively short periods of repose. Short repose intervals are indicated by the absence of weathering, erosion, sedimentation, and magnetic reversals, in addition to age constraints.

Distinct phases of volcanism, characterized by changes in the chemistry of the basalts, occur during the construction of some oceanic

TABLE 6. SUMMARY OF THE ARCHITECTURE OF THREE MAJOR OCEANIC PLATEAUS

Wrangellia	Ontong Java	Caribbean
(overlying flood basalts)	*(overlying flood basalts)*	*(overlying flood basalts)*
Vancouver Island and Alaska Primarily limestone, chert, shale (Late Triassic to Early Jurassic)	Lower Aptian (Lower Cretaceous) to Miocene pelagic sediment (>1000 m)	Late Cretaceous and Tertiary pelagic carbonate in Caribbean Sea
<2 km thick on VI, ~2 km thick in areas of Alaska	Pelagic sediment deposits in low-energy, submarine environment above the CCD	Foraminifera-nannofossil ooze; rare shallow water fossils
Overlying limestone grades upward from shallow to deeper water facies		Silicified limestone and chert less common
Late Carnian to early Nornian (Triassic) fossils in overlying limestone		
Thin (<25 cm) layer of siltstone immediately overlying basalt	Nannofossil studies reveal six unconformities	Black shales indicative of oceanic anoxia
Little evidence of erosion between basalt and overlying limestone		Cenomanian-Turonian boundary extinction event linked to plateau formation
Triassic-Jurassic boundary preserved in shale in Alaska	Oceanic Anoxic Event 1a suggested to be result of eruption of plateau basalts	
(flood basalts)	*(flood basalts)*	*(flood basalts)*
Single eruption phase (231–225 Ma)	Multiple eruption phases, main initial episode (122 ± 3 Ma) ca. 90 Ma volcanism is minor	Multiple eruption phases, main initial episode (93–89 Ma) Minor volcanism at 76–72 Ma
High proportion of subaerial flows (~40% on VI, ~90% in Alaska)	Low proportion of subaerial flows	Low proportion of subaerial flows
Very little sediment between flows (high eruption rate)	Very little sediment between flows (high eruption rate)	Very little sediment between flows (high eruption rate)
Initial eruptions in deep water (VI)	Formed mostly in deep water (mostly below CCD)	Deep- and shallow-water eruptions
Rare dikes, sills abundant near base	Rare dikes, sills present on Malaita (1–50 m thick; Solomon Islands)	Rare dikes, sills?
Continental detritus absent	Continental material absent	Continental material absent
Predominantly tholeiitic basalt (no alkalic basalt or felsic lavas)	Predominantly tholeiitic basalt (no alkalic basalt or felsic lavas)	Predominantly tholeiitic basalt (no alkalic basalt or felsic lavas)
High-MgO pillow lavas in submarine section	High-MgO picritic lavas present	High-MgO picritic lavas present
Submarine flows mostly pillowed with lesser massive, jointed flows	Submarine flows mostly pillowed with rare massive flows	
Rare plagioclase-megacrystic basalt in upper stratigraphy		
Rare spheruloidal basalt	Rare spheruloidal basalt	Evidence of erosion in shallow-marine environment
Increasing vesicularity and volcaniclastics upward in stratigraphy	Amygdules are rare	Volcaniclastics in Caribbean indicate subaerial and/or shallow-marine eruptions
Vancouver Island-Karmutsen Formation (~6000 m)	Rare 1–5 mm noncalcareous pelagic sediment between flows	Coral fossils in volcanic tuffs within Columbia basalts (shallow water)
Local interflow limestone in upper stratigraphy	Volcaniclastic sequences, oxidized horizons, wood fragments indicate subaerial and/or shallow marine eruptions	Curaçao basalt stratigraphy >5 km thick (picrite lower in section, evolved basalt higher in succession, >2 km hyaloclastite)
Upper—subaerial basalt flows (>2500 m on CVI, <1500 m on NVI)		
Middle—pillow breccia and hyaloclastite (400–1500 m on NVI)	Thin (<1 m) and thick (>50 m) flows	Picritic and tholeiitic flows commonly separated by hyaloclastite on Curacao
Keogh Lake picrite (pillow lavas, NVI)	Columnar jointing rare in massive flows	
Lower—pillowed and massive submarine flows (>2500 m)	Smooth upper surface capped by several large seamounts	Stratigraphy (based on Kerr et al., 1998): Thin pelagic sediments
	Trap-like topography on Malaita	Extrusive sections-homogeneous pillow lavas, intrusive sheets (sills)
Alaska-Nikolai Formation (~3500 m)	95% flows <25 m thick, 50% flows 5–10 m thick	Heterogeneous picrite, komatiite, and basalt flows
Predominantly subaerial basalt flows		Intrusive sections—isotropic gabbro and gabbronorite
Pillow basalt (<800 m) in Alaska Range		Layered gabbroic rocks
Flow conglomerate, pillow breccia along base in Wrangell Mtns (<100 m)	*(deepest level of exposure)*	Ultramafic rocks—dunite with bands of pyroxenite and lherzolite

(*continued*)

TABLE 6. SUMMARY OF THE ARCHITECTURE OF THREE MAJOR OCEANIC PLATEAUS (continued)

Wrangellia	Ontong Java	Caribbean
(stratigraphically beneath flood basalts)	*(stratigraphy beneath basalts is not exposed on Malaita)*	*(stratigraphically beneath flood basalts)*
Middle Triassic *Daonella* beds and mafic sills	Seismic and magnetic surveys indicate:	
Silicified shale, chert, minor limestone	Mafic intrusions beneath the flood basalts	Layered and isotropic gabbros and ultramafic plutonic rocks exposed in Columbia (cumulates from flood basalt volcanism)
Evidence of erosion (rounded clasts) of sequences beneath Nikolai	Basalts erupted on oceanic crust, possibly near spreading ridge	
Mafic intrusions related to flood basalts in underlying sedimentary sequences	Estimated total thickness of extrusive and intrusives of ~33 km	
Formation of laterally discontinuous grabens along base in Yukon		Basalts erupted on oceanic crust, possibly near spreading ridge
Vancouver Island		Estimated total thickness of extrusive and intrusives of ~20 km
Mississippian–Early Permian limestone and argillite (Buttle Lake Group)		
Devonian–Early Mississippian arc-derived volcanic rocks (Sicker Group)		
Mafic sills and intrusive suites		
Alaska (Skolai Group)		
Early Permian bioclastic limestone, chert, shale (Hasen Creek Fm.)		
Pennsylvannian–Early Permian arc-derived volcanics (Station Creek Fm.)		
(deepest level of exposure)		*(deepest level of exposure)*

Note: CCD is carbonate compensation depth. NVI, northern Vancouver Island; CVI, central Vancouver Island; Fm, Formation. See supplementary data files for references.

plateaus and many continental flood basalts. In the latter, three main phases of volcanism include initial low-volume transitional to alkalic eruptions, a main phase of large volume of tholeiitic flows that produced large flow fields from fissure eruptions, and a waning phase of decreased-volume eruptions from widely distributed, localized volcanic centers with higher silica and/or alkali lavas and explosivity (Jerram and Widdowson, 2005). In contrast, oceanic plateaus appear to largely form during a single, main tholeiitic phase, such as observed for Wrangellia, although both the Ontong Java and Caribbean Plateaus reveal distinct phases of late-stage volcanism (Table 6). The evolution of the Ontong Java, Manihiki, and Hikurangi plateaus (Fig. 1), which are perhaps dispersed parts of a single giant oceanic plateau (Taylor, 2006), show similarities with a main tholeiitic stage (ca. 126–116 Ma) followed by late-stage volcanism lasting more than 30 Myr (Davy et al., 2008). The late-stage volcanism on Hikurangi and Manihiki includes seamounts and volcanic ridges that are mostly alkalic in composition, whereas late-stage volcanism on Ontong Java is mostly tholeiitic (although alkalic rocks are present; Hoernle et al., 2008). To date, there is no evidence for a clear gap in volcanism in the formation of the Wrangellia oceanic plateau, although additional high-precision geochronology is required to better evaluate the onset and termination of magmatism. There is also no evidence for, or trend toward, alkalic compositions from basaltic sections sampled on Vancouver Island and in Yukon and Alaska (Greene et al., 2008, 2009a, 2009b), even for samples taken from the uppermost stratigraphic sections just below covering sedimentary rocks. Perhaps parts of the Wrangellia plateau are missing or are not exposed, or Wrangellia may represent a purely tholeiitic large igneous province formed during a single-stage (<5 Myr) interval of time.

The high eruption rates, relatively short periods of repose, and basaltic lava compositions of the Wrangellia and other oceanic plateaus are comparable to those of continental flood basalts, which have estimated eruption rates orders of magnitude greater than present-day hotspots such as Hawaii (e.g., Thordarson and Self, 1996; White et al., 2006). The volumetric output of flow fields in continental flood basalts, which is likely comparable for oceanic plateaus, is on the order of hundreds to thousands of cubic meters per second, and individual flow fields persist for years to perhaps more than a decade (although volumes of individual eruption events can be highly variable; Jerram, 2002). For example, the flow rate estimated for the Roza flow field in the Columbia River Basalt Group (~4000 m^3/s) is orders of magnitude higher than the flow of lava during the past 26 yr on Kilauea Volcano on the island of Hawaii (~2 m^3/s; <6 m^3/s; Heliker and Mattox, 2003). The higher sustained flow rates for the tholeiitic basaltic lavas that dominated oceanic plateaus produce compound flow fields as opposed to shield-like features that form from the lower volume eruptions on Hawaiian, and other hotspot, volcanoes. The morphology of flows in oceanic plateaus is also distinct from flows on Hawaiian volcanoes. Oceanic plateaus consist of thick (10–50 m), tabular and laterally extensive flows extending tens of kilometers, whereas Hawaiian volcanoes form thin (<5 m) lobes with large local variation and features like volcanic cones, craters, and channels. Despite comparably high estimates of eruption rates for modern eruptions at ocean island hotpots over brief periods (e.g., Laki, 1983–1984; Self et al., 1997), there is no modern analogue for the formation of submarine sections of oceanic plateaus.

CONCLUSIONS

The volcanic stratigraphy of the obducted Wrangellia flood basalts records the construction of a major oceanic plateau and provides a rare view of the preeruption, syneruption, and posteruption phases and paleoenvironments of an oceanic plateau that originated from a plume-related magmatic event not associated with mid-ocean ridge–controlled processes. The Wrangellia basalts are now exposed over ~27 × 10^3 km^2 in Alaska, Yukon, and British Columbia (Vancouver Island and Queen Charlotte Islands) along the western edge of North America, although the original extent was significantly greater. Geochronologic, paleontological, and magnetostratigraphic constraints indicate that

volcanism in Northern and Southern Wrangellia occurred ca. 230–225 Ma.

In Northern Wrangellia, the basalts in Alaska (~3.5 km thick) and Yukon are bounded by Middle to Late Triassic marine sediments and unconformably overlie Pennsylvanian and Permian marine sediments and volcanic arc sequences (ca. 312–280 Ma). The earliest flows were emplaced in a shallow-marine environment, but the main phase of volcanism consisted of compound pahoehoe flow fields that form a tabular, shingled architecture with high-Ti basalts overlying low-Ti basalts. Grabens formed along the base of Wrangellia basalts in Yukon.

In Southern Wrangellia, basalts on Vancouver Island (~6 km thick) are bounded by Middle to Late Triassic marine sediments and unconformably overlie a basement of Devonian–Mississippian arc rocks and Mississippian–Permian marine sedimentary strata. Early growth of the volcanic stratigraphy on Vancouver Island was dominated by extrusion of pillow lavas and intrusion of sills into sedimentary strata. The plateau grew from the ocean floor and accumulated >3000 m of submarine flows, which were overlain by 400–1500 m of hyaloclastite and minor pillow basalt before the plateau breached sea level. The hyaloclastite formed primarily by quench fragmentation of effusive flows under low hydrostatic pressure. The plateau then grew above sea level as >1500 m of subaerial flows were emplaced. The plateau subsided during its construction and intervolcanic sedimentary lenses formed in shallow water in local areas as eruptions waned. After volcanism ceased, the plateau continued to subside for more than 25 Myr and was overlain by hundreds of meters to >1000 m of limestone and siliciclastic deposits.

Wrangellia holds keys to understanding some of the important questions about the development of oceanic plateaus, the time scale of eruptions, mantle properties during large-scale melting events, and possible effects on the environment.

ACKNOWLEDGMENTS

This manuscript was influenced by discussions with Travis Hudson and material that he provided. We are grateful to Jeff Trop for his advice. Jeanine Schmidt and Peter Bittenbender were very helpful with data and ideas about Alaskan geology. Don Carlisle thoughtfully provided maps and notes that helped with field work on Vancouver Island. Andrew Caruthers and Chris Ruttan helped with field work on Vancouver Island. David Brew was very helpful with information about southeast Alaska. Journal reviews by Lincoln Hollister and Colin Shaw were especially useful in helping us focus the information and ideas presented in this paper. Funding was provided by research grants from the British Columbia Geological Survey and Yukon Geological Survey, the Rocks to Riches Program administered by the British Columbia and Yukon Chamber of Mines, and Natural Sciences and Engineering Research Council Discovery Grants to James Scoates and Dominique Weis. A. Greene was supported by a University Graduate Fellowship at the University of British Columbia.

REFERENCES CITED

Armstrong, A.K., MacKevett, E.M., Jr., and Silberling, N.J., 1969, The Chitistone and Nizina limestones of part of the southern Wrangell Mountains—A preliminary report stressing carbonate petrography and depositional environments: U.S. Geological Survey Professional Paper 650-D, p. D49–D62.

Beard, J.S., and Barker, F., 1989, Petrology and tectonic significance of gabbros, tonalites, shoshonites, and anorthosites in a late Paleozoic arc-root complex in the Wrangellia Terrane, southern Alaska: Journal of Geology, v. 97, p. 667–683, doi: 10.1086/629351.

Ben-Avraham, Z., Nur, A., Jones, D.L., and Cox, A., 1981, Continental accretion: From oceanic plateaus to allochthonous terranes: Science, v. 213, p. 47–54, doi: 10.1126/science.213.4503.47.

Bittenbender, P.E., Bean, K.W., and Gensler, E.G., 2003, Mineral Investigations in the Delta River Mining District, east-central Alaska 2001–2002: U.S. Bureau of Land Management-Alaska, Open-File Report 91, 88 p.

Bittenbender, P.E., Bean, K.W., Kurtak, J.M., and Deninger, J., Jr., 2007, Mineral assessment of the Delta River Mining District area, east-central Alaska: U.S. Bureau of Land Management-Alaska Technical Report 57, 676 p., http://www.blm.gov/pgdata/etc/medialib/blm/ak/aktest/tr.Par.86412.File.dat/BLM_TR57.pdf.

Blodgett, R.B., 2002, Paleontological inventory of the Amphitheater Mountains, Mt. Hayes A-4 and A-5 Quadrangles, south-central Alaska: Alaska Division of Geological and Geophysical Surveys Report of Investigations 2002–3, 11 p.

Brandon, M.T., Orchard, M.J., Parrish, R.R., Sutherland-Brown, A., and Yorath, C.J., 1986, Fossil ages and isotopic dates from the Paleozoic Sicker Group and associated intrusive rocks, Vancouver Island, British Columbia: Current Research, Part A: Geological Survey of Canada Paper 86–1A, p. 683–696.

Breitsprecher, K. and Mortensen, J.K., 2004a, BCAge 2004A-1 - a database of isotopic age determinations for rock units from British Columbia: British Columbia Ministry of Energy and Mines, Geological Survey, Open File 2004-3 (Release 3.0), 7757 records.

Breitsprecher, K., and Mortensen, J.K., comps., 2004b, YukonAge 2004: A database of isotopic age determinations for rock units from Yukon Territory: Yukon Geological Survey, CD-ROM.

Burns, L.E., and Clautice, K.H., 2003, Portfolio of aeromagnetic and resistivity maps of the southern Delta River area, east-central Alaska: Alaska Division of Geological and Geophysical Surveys Geophysical Report 2003–8, 16 p.

Burns, L.E., U.S. Bureau of Land Management, Fugro Airborne Surveys, and Stevens Exploration Management Corporation, 2003, Color shadow magnetic map of the southern Delta River area, east-central Alaska: Alaska Division of Geological and Geophysical Surveys Geophysical Report 2003–5-1C, 2 sheets, scale 1:63,360.

Campbell, I.H., and Griffiths, R.W., 1990, Implications of mantle plume structure for the evolution of flood basalts: Earth and Planetary Science Letters, v. 99, p. 79–93, doi: 10.1016/0012-821X(90)90072-6.

Campbell, S.W., 1981, Geology and genesis of copper deposits and associated host rocks in and near the Quill Creek area, southwestern Yukon [Ph.D. thesis]: Vancouver, University of British Columbia, 215 p.

Carlisle, D., 1963, Pillow breccias and their aquagene tuffs, Quadra Island, British Columbia: Journal of Geology, v. 71, p. 48–71, doi: 10.1086/626875.

Carlisle, D., 1972, Late Paleozoic to Mid-Triassic sedimentary-volcanic sequence on Northeastern Vancouver Island: Geological Society of Canada Report of Activities 72–1, Part B, p. 24–30.

Carlisle, D., and Suzuki, T., 1974, Emergent basalt and submergent carbonate-clastic sequences including the Upper Triassic Dilleri and Welleri zones on Vancouver Island: Canadian Journal of Earth Sciences, v. 11, p. 254–279.

Cho, M., and Liou, J.G., 1987, Prehnite-pumpellyite to greenschist facies transition in the Karmutsen metabasites, Vancouver Island, B.C: Journal of Petrology, v. 28, p. 417–443.

Clowes, R.M., Zelt, C.A., Amor, J.R., and Ellis, R.M., 1995, Lithospheric structure in the southern Canadian Cordillera from a network of seismic refraction lines: Canadian Journal of Earth Sciences, v. 32, p. 1485–1513.

Coffin, M.F., 1992, Subsidence of the Kerguelen Plateau: The Atlantis concept, *in* Wise, S.W., Jr., et al., Proceedings of Ocean Drilling Program, Scientific results, Volume 120: College Station, Texas, Ocean Drilling Program, p. 945–949.

Coffin, M.F., and Eldholm, O., 1994, Large igneous provinces: Crustal structure, dimensions, and external consequences: Reviews of Geophysics, v. 32, no. 1, p. 1–36, doi: 10.1029/93RG02508.

Cohen, B.A., 2004, Can granulite metamorphic conditions reset $^{40}Ar/^{39}Ar$ ages in lunar rocks?: Lunar and Planetary Science Conference XXXV, abs. 1009.

Coney, P.J., Jones, D.L., and Monger, J.W.H., 1980, Cordilleran suspect terranes: Nature, v. 288, no. 5789, p. 329, doi: 10.1038/288329a0.

Courtillot, V.E., and Renne, P.R., 2003, On the ages of flood basalt events: Comptes Rendus Geoscience, v. 335, p. 113–140, doi: 10.1016/S1631-0713(03)00006-3.

Csejtey, B., Jr., Cox, D.P., Evarts, R.C., Stricker, G.D., and Foster, H.L., 1982, The Cenozoic Denali fault system and the Cretaceous accretionary development of southern Alaska: Journal of Geophysical Research, v. 87, p. 3741–3754, doi: 10.1029/JB087iB05p03741.

Davy, B., Hoernle, K., and Werner, R., 2008, Hikurangi Plateau: Crustal structure, rifted formation, and Gondwana subduction history: Geochemistry Geophysics Geosystems, v. 9, Q07004, doi: 10.1029/2007GC001855.

Detrick, R.S., Sclater, J.G., and Thiede, J., 1977, The subsidence of aseismic ridges: Earth and Planetary Science Letters, v. 34, p. 185–198, doi: 10.1016/0012-821X(77)90003-6.

Dodds, C.J., and Campbell, R.B., 1988, Potassium-argon ages of mainly intrusive rocks in the Saint Elias Mountains, Yukon and British Columbia: Geological Society of Canada Paper 87–16, 43 p.

Frey, F.A., and 27 others, 2000, Origin and evolution of a submarine large igneous province: The Kerguelen Plateau and Broken Ridge, southern Indian Ocean: Earth and Planetary Science Letters, v. 176, p. 73–89, doi: 10.1016/S0012-821X(99)00315-5.

Furin, S., Preto, N., Rigo, M., Roghi, G., Gianolla, P., Crowley, J.L., and Bowring, S.A., 2006, High-precision U-Pb zircon age from the Triassic of Italy: Implications for the Triassic time scale and the Carnian origin of calcareous nannoplankton and dinosaurs: Geology, v. 34, p. 1009–1012, doi: 10.1130/G22967A.1.

Garcia, M.O., Haskins, E.H., Stolper, E.M., and Baker, M., 2007, Stratigraphy of the Hawai'i Scientific Drilling Project core (HSDP2): Anatomy of a Hawaiian shield volcano: Geochemistry Geophysics Geosystems, v. 8, Q02G20, doi: 10.1029/2006GC001379.

Gardner, M.C., Bergman, S.C., Cushing, G.W., MacKevett, E.M., Jr., Plafker, G., Campbell, R.B., Dodds, C.J., McClelland, W.C., and Mueller, P.A., 1988, Pennsylvanian pluton stitching of Wrangellia and the Alexander terrane, Wrangell Mountains, Alaska: Geology, v. 16, p. 967–971, doi: 10.1130/0091-7613(1988)016<0967:PPSOWA>2.3.CO;2.

Glen, J.M.G., Schmidt, J.M., and Morin, R., 2007a, Gravity and magnetic studies of the Talkeetna Mountains, Alaska: Constraints on the geological and tectonic interpretation of southern Alaska, and implications for mineral exploration, *in* Ridgway, K.D., et al., eds., Tectonic growth of a collisional continental margin: Crustal evolution of southern Alaska: Geological Society of America Special Paper 431, p. 593–622.

Glen, J.M.G., Schmidt, J.M., Pellerin, L., O'Niell, M., and McPhee, D.K., 2007b, Crustal structure of Wrangellia and adjacent terranes inferred from geophysical studies along a transect through the northern Talkeetna Mountains, *in* Ridgway, K.D., et al., eds., Tectonic growth of a collisional continental margin: Crustal evolution of southern Alaska: Geological Society of America Special Paper 431, p. 21–42.

Gradstein, F.M., Ogg, J.G., and Smith, A.G., eds., 2004, A geologic time scale 2004: Cambridge, Cambridge University Press, 610 p.

Grantz, A., Jones, D.L., and Lanphere, M.A., 1966, Stratigraphy, paleontology, and isotopic ages of upper Mesozoic rocks in the southwestern Wrangell Mountains, Alaska, *in* U.S. Geological Survey Staff, Geological Survey research 1966: U.S. Geological Survey Professional Paper 550-C, p. 39–47.

Greene, A.R., Scoates, J.S., Nixon, G.T., and Weis, D., 2006, Picritic lavas and basal sills in the Karmutsen flood basalt province, Wrangellia, northern Vancouver Island, *in* Grant, B., ed., Geological fieldwork 2005: British Columbia Ministry of Energy, Mines and Petroleum Resources Paper 2006–1, p. 39–52.

Greene, A.R., Scoates, J.S., and Weis, D., 2008, Wrangellia flood basalts in Alaska: A record of plume-lithosphere interaction in a Late Triassic accreted oceanic plateau: Geochemistry Geophysics Geosystems, v. 9, Q12004, doi: 10.1029/2008GC002092.

Greene, A.R., Scoates, J.S., Weis, D., and Israel, S., 2009a, Geochemistry of flood basalts from the Yukon (Canada) segment of the accreted Wrangellia oceanic plateau: Lithos, v. 110, p. 1–19, doi: 10.1016/j.lithos.2008.11.010.

Greene, A.R., Scoates, J.S., Weis, D., Nixon, G.T., and Kieffer, B., 2009b, Melting history and magmatic evolution of basalts and picrites from the accreted Wrangellia oceanic plateau, Vancouver Island, Canada: Journal of Petrology, v. 50, p. 467–505, doi: 10.1093/petrology/egp008.

Harrison, T.M., and McDougall, I., 1981, Excess ^{40}Ar in metamorphic rocks from Broken Hill, New South Wales: Implications for ^{40}Ar/^{39}Ar age spectra and the thermal history of the region: Earth and Planetary Science Letters, v. 55, p. 123–149, doi: 10.1016/0012-821X(81)90092-3.

Heliker, C.C., and Mattox, T.N., 2003, The first two decades of the Pu'u 'Ō'ō-Kūpaianaha eruption: Chronology and selected bibliography, *in* Heliker, C., et al., eds., The Pu'u 'Ō'ō-Kūpaianaha eruption of Kīlauea Volcano, Hawaii: The first 20 years: U.S. Geological Survey Professional Paper 1676, p. 1–28.

Hillhouse, J.W., 1977, Paleomagnetism of the Triassic Nikolai Greenstone, McCarthy Quadrangle, Alaska: Canadian Journal of Earth Sciences, v. 14, p. 2578–2592, doi: 10.1139/e77-223.

Hillhouse, J.W., and Gromme, C.S., 1984, Northward displacement and accretion of Wrangellia: New paleomagnetic evidence from Alaska: Journal of Geophysical Research, v. 89, p. 4461–4467, doi: 10.1029/JB089iB06p04461.

Hodges, K.V., 2003, Geochronology and thermochronology in orogenic systems, *in* Rudnick, R., ed., The crust, *in* Holland, H.D., and Turekian, K.K., eds., Treatise on geochemistry, Volume 3: Oxford, Elsevier-Pergamon, p. 263–292.

Hoernle, K., Hauff, F., Werner, R., van den Bogaard, P., Timm, C., Coffin, M., Mortimer, N., and Davy, B., 2008, A similar multi-stage geochemical evolution for the Manihiki, Hikurangi and Ontong Java Plateaus?: Eos (Transactions, American Geophysical Union), v. 89, fall meeting supplement, abs. V23H–05.

Hollister, L.S., and Andronicos, C.L., 2006, Formation of new continental crust in western British Columbia during transpression and transtension: Earth and Planetary Science Letters, v. 249, p. 29–38, doi: 10.1016/j.epsl.2006.06.042.

Hudson, T., 1983, Calk-alkaline plutonism along the Pacific Rim of southern Alaska, *in* Roddick, J.A., ed., Circum-Pacific plutonic terranes: Geological Society of America Memoir 159, p. 159–169.

Irving, E., and Yole, R.W., 1972, Paleomagnetism and kinematic history of mafic and ultramafic rocks in fold mountain belts: Ottawa, Canada, Publications of the Earth Physics Branch, v. 42, p. 87–95.

Israel, S., 2004, Geology of southwestern Yukon: Yukon Geological Survey Open File 2004–16, scale 1:250,000.

Israel, S., Tizzard, A., and Major, J., 2006, Bedrock geology of the Duke River area, parts of NTS 115G/2, 3, 4, 6 and 7, southwestern Yukon, *in* Emond, D.S., et al., eds., Yukon exploration and geology 2004: Whitehorse, Yukon Geological Survey, p. 139–154.

Ito, G., and Clift, P.D., 1998, Subsidence and growth of Pacific Cretaceous plateaus: Earth and Planetary Science Letters, v. 161, p. 85–100, doi: 10.1016/S0012-821X(98)00139-3.

Jerram, D.A., 2002, Volcanology and facies architecture of flood basalts, *in* Menzies, M.A., et al., eds., Volcanic rifted margins: Geological Society of America Special Paper 362, p. 119–132.

Jerram, D.A., and Widdowson, M., 2005, The anatomy of continental flood basalt provinces: Geological constraints on the processes and products of flood volcanism: Lithos, v. 79, p. 385–405, doi: 10.1016/j.lithos.2004.09.009.

Jones, D.L., Silberling, N.J., and Hillhouse, J., 1977, Wrangellia—A displaced terrane in northwestern North America: Canadian Journal of Earth Sciences, v. 14, p. 2565–2577, doi: 10.1139/e77-222.

Jones, J.G., 1969, Pillow lavas as depth indicators: American Journal of Science, v. 267, p. 181–195.

Juras, S.J., 1987, Geology of the polymetallic volcanogenic Buttle Lake Camp, with emphasis on the Prince Hillside, Vancouver Island, British Columbia, Canada [Ph.D. thesis]: Vancouver, University of British Columbia, 279 p.

Katvala, E.C., and Henderson, C.M., 2002, Conodont sequence biostratigraphy and paleogeography of the Pennsylvanian-Permian Mount Mark and Fourth Lake Formations, southern Vancouver Island, *in* Hills, L.V., et al., eds., Carboniferous and Permian of the world: Canadian Society of Petroleum Geologists Memoir 19, p. 461–478.

Kent, D.V., and Olsen, P.E., 1999, Astronomically tuned geomagnetic polarity timescale for the Late Triassic: Journal of Geophysical Research, v. 104, no. B6, p. 12,831–12,841, doi: 10.1029/1999JB900076.

Kerr, A.C., 2003, Oceanic plateaus, *in* Holland, H.D., and Turekian, K.K., eds., Treatise on geochemistry, Volume 3: Oxford, Elsevier-Pergamon, p. 537–565.

Kerr, A.C., Tarney, J., Nivia, A., Marriner, G.F., and Saunders, A.D., 1998, The internal structure of oceanic plateaus: Inferences from obducted Cretaceous terranes in western Colombia and the Caribbean: Tectonophysics, v. 292, p. 173–188, doi: 10.1016/S0040-1951(98)00067-5.

Kokelaar, P., 1986, Magma-water interactions in subaqueous and emergent basaltic volcanism: Bulletin of Volcanology, v. 48, p. 275–289, doi: 10.1007/BF01081756.

Koppers, A.A.P., 2002, ArArCALC—Software for ^{40}Ar/^{39}Ar age calculations: Computers & Geosciences, v. 28, p. 605–619, doi: 10.1016/S0098-3004(01)00095-4.

Lanphere, M.A., and Dalrymple, G.B., 1976, Identification of excess ^{40}Ar by the ^{40}Ar/^{39}Ar age spectrum technique: Earth and Planetary Science Letters, v. 32, p. 141–148, doi: 10.1016/0012-821X(76)90052-2.

Lanphere, M.A., and Dalrymple, G.B., 2000, First-principles calibration of ^{38}Ar tracers: Implications for the ages of ^{40}Ar/^{39}Ar fluence monitors: U.S. Geological Survey, 1621.

Lassiter, J.C., 1995, Geochemical investigations of plume-related lavas: Constraints on the structure of mantle plumes and the nature of plume/lithosphere interactions [Ph.D. thesis]: Berkeley, University of California, 231 p.

MacKevett, E.M., Jr., 1978, Geologic map of the McCarthy Quadrangle, Alaska: U.S. Geological Survey Miscellaneous Geological Investigations Map I-1032, scale 1:250,000.

MacKevett, E.M., Jr., Berg, H.C., Plafker, G., and Jones, D.L., 1964, Prelimary geologic map of the McCarthy C-4 Quadrangle, Alaska: U.S. Geological Survey Miscellaneous Geological Investigations Map I-423, scale 1:63,360.

Mahoney, J.J., and Coffin, M.F., eds., 1997, Large igneous provinces: Continental, oceanic, and planetary flood volcanism: American Geophysical Union Geophysical Monograph 100, 438 p.

Mahoney, J.J., Duncan, R.A., Tejada, M.L.G., Sager, W.W., and Bralower, T.J., 2005, Jurassic-Cretaceous boundary age and mid-ocean-ridge-type mantle source for Shatsky Rise: Geology, v. 33, p. 185–188, doi: 10.1130/G21378.1.

Massey, N.W.D., 1995, Geology and mineral resources of the Alberni-Nanaimo Lakes sheet, Vancouver Island 92F/1W, 92F/2E, and part of 92F/7E: British Columbia Ministry of Energy, Mines and Petroleum Resources Paper 1992–2, 132 p.

Massey, N.W.D., and Friday, S.J., 1988, Geology of the Chemainus River-Duncan area, Vancouver Island (92C/16; 92B/13), *in* Geological fieldwork 1987: British Columbia Ministry of Energy, Mines and Petroleum Resources Paper 1988–1, p. 81–91.

Massey, N.W.D., MacIntyre, D.G., Desjardins, P.J., and Cooney, R.T., 2005a, Digital geology map of British Columbia: Tile NM9 Mid Coast, B.C: British Columbia Ministry of Energy and Mines Geofile 2005–2.

Massey, N.W.D., MacIntyre, D.G., Desjardins, P.J., and Cooney, R.T., 2005b, Digital geology map of British Columbia: Tile NM10 Southwest B.C: British Columbia Ministry of Energy and Mines Geofile 2005–3.

McClelland, W.C., Gehrels, G.E., and Saleeby, J.B., 1992, Upper Jurassic–Lower Cretaceous basinal strata along the Cordilleran margin: Implication for the accretionary history of the Alexander-Wrangellia-Peninsular terranes: Tectonics, v. 11, p. 823–835, doi: 10.1029/92TC00241.

Monger, J.W.H., and Journeay, J.M., 1994, Basement geology and tectonic evolution of the Vancouver region, *in* Monger, J.W.H., ed., Geology and geological hazards of the Vancouver region, southwestern British Columbia: Geological Survey of Canada Bulletin 481, p. 3–25.

Monger, J.W.H., Price, R.A., and Tempelman-Kluit, D.J., 1982, Tectonic accretion and the origin of the two major metamorphic and plutonic welts in the Canadian Cordillera: Geology, v. 10, p. 70–75, doi: 10.1130/0091-7613(1982)10<70:TAATOO>2.0.CO;2.

Moore, J.G., and Clague, D.A., 1992, Volcano growth and evolution of the island of Hawaii: Geological Society of America Bulletin, v. 104, p. 1471–1484, doi: 10.1130/0016-7606(1992)104<1471:VGAEOT>2.3.CO;2.

Mortensen, J.K., and Hulbert, L.J., 1992, A U-Pb zircon age for a Maple Creek gabbro sill, Tatamagouche Creek area, southwestern Yukon Territory, *in* Radiogenic age and isotopic studies: Report 5: Geological Survey of Canada Paper 91-2, p. 175–179 p.

Muller, J.E., 1967, Kluane Lake map area, Yukon Territory (115G, 115F/E 1/2): Geological Survey of Canada Memoir 340, 137 p.

Muller, J.E., 1977, Geology of Vancouver Island: Geological Survey of Canada Open File Map 463.

Newton, C.R., 1983, Paleozoogeographic affinities of Norian bivalves from the Wrangellian, Peninsular, and Alexander terranes, northwestern North America, *in* Stevens, C.H., ed., Pre-Jurassic rocks in western North American suspect terranes: Pacific Section, Society of Economic Paleontologists and Mineralogists Book 32, p. 37–48.

Nixon, G.T., and Orr, A.J., 2007, Recent revisions to the early Mesozoic stratigraphy of Northern Vancouver Island (NTS 102I; 092L) and metallogenic implications, British Columbia, *in* Grant, B., ed., Geological fieldwork 2006: British Columbia Ministry of Energy, Mines and Petroleum Resources Paper 2007-1, p. 163–177.

Nixon, G.T., Laroque, J., Pals, A., Styan, J., Greene, A.R., and Scoates, J.S., 2008, High-Mg lavas in the Karmutsen flood basalts, northern Vancouver Island (NTS 092L): Stratigraphic setting and metallogenic significance, *in* Grant, B., ed., Geological fieldwork 2007: British Columbia Ministry of Energy, Mines and Petroleum Resources Paper 2008-1, p. 175–190.

Nokleberg, W.J., Aleinikoff, J.N., Dutro, J.T.J., Lanphere, M.A., Silberling, N.J., Silva, S.R., Smith, T.E., and Turner, D.L., 1992, Map, tables, and summary fossil and isotopic age data, Mount Hayes quadrangle, eastern Alaska Range, Alaska: U.S. Geological Survey Miscellaneous Field Studies Map 1996-D, scale 1:250,000.

Nokleberg, W.J., Plafker, G., and Wilson, F.H., 1994, Geology of south-central Alaska, *in* Plafker, G., and Berg, H.C., eds., The geology of Alaska: Boulder, Colorado, Geological Society of America, The geology of North America, v. G-1, p. 311–366.

Ogg, J.G., 2004, The Triassic Period, *in* Gradstein, F.M., et al., eds., A geologic time scale 2004: Cambridge, Cambridge University Press, p. 271–306.

Orchard, M.J., 1986, Conodonts from western Canadian chert: Their nature, distribution and stratigraphic application, *in* Austin, R.L., ed., Conodonts, investigative techniques and applications: Proceeding of the Fourth European Conodont Symposium (ECOS IV): London, U.K., Ellis-Horwood, p. 96–121.

Parrish, R.R., and McNicoll, V.J., 1992, U-Pb age determinations from the southern Vancouver Island area, British Columbia, *in* Radiogenic age and isotopic studies, Report 5: Geological Survey of Canada Paper 91-2, p. 79–86.

Petterson, M.G., 2004, The geology of north and central Malaita, Solomon Islands: The thickest and most accessible part of the world's largest (Ontong Java) oceanic plateau, *in* Fitton, J. G., et al., eds., Origin and evolution of the Ontong Java Plateau: Geological Society of London Special Publication 229, p. 63–81.

Plafker, G., and Berg, H.C., 1994, Overview of the geology and tectonic evolution of Alaska, *in* Plafker, G., and Berg, H.C., eds., The geology of Alaska: Boulder, Colorado, Geological Society of America, The geology of North America, v. G-1, p. 989–1021.

Plafker, G., and Hudson, T., 1980, Regional implications of the Upper Triassic metavolcanic and metasedimentary rocks on the Chilkat Peninsula, southeastern Alaska: Canadian Journal of Earth Sciences, v. 17, p. 681–689.

Plafker, G., Nokleberg, W.J., and Lull, J.S., 1989, Bedrock geology and tectonic evolution of the Wrangellia, Peninsular, and Chugach terranes along the Trans-Alaskan Crustal Transect in the northern Chugach Mountains and southern Copper River basin, Alaska: Journal of Geophysical Research, v. 94, p. 4255–4295.

Plafker, G., Moore, J.C., and Winkler, G.R., 1994, Geology of the southern Alaska margin, *in* Plafker, G., and Berg, H.C., eds., The geology of Alaska: Boulder, Colorado, Geological Society of America, The geology of North America, v. G-1, p. 389–449.

Prichard, R.A., 2003, Project report of the airborne geophysical survey for the southern Delta River area, east-central Alaska: Alaska Division of Geological and Geophysical Surveys Geophysical Report 2003-7, 2 sheets, scale 1:63,360, 252 p.

Read, P.B., and Monger, J.W.H., 1976, Pre-Cenozoic volcanic assemblages of the Kluane and Alsek Ranges, southwestern Yukon Territory: Geological Survey of Canada Open File Report 381, 96 p.

Renne, P.R., Swisher, C.C., III, Deino, A.L., Karner, D.B., Owens, T., and DePaolo, D.J., 1998, Intercalibration of standards, absolute ages and uncertainties in $^{40}Ar/^{39}Ar$ dating: Chemical Geology, v. 145, p. 117–152, doi: 10.1016/S0009-2541(97)00159-9.

Richards, M.A., Jones, D.L., Duncan, R.A., and DePaolo, D.J., 1991, A mantle plume initiation model for the Wrangellia flood basalt and other oceanic plateaus: Science, v. 254, p. 263–267, doi: 10.1126/science.254.5029.263.

Ridgway, K.D., Trop, J.M., Nokleberg, W.J., Davidson, C.M., and Eastham, K.R., 2002, Mesozoic and Cenozoic tectonics of the eastern and central Alaska Range: Progressive basin development and deformation in a suture zone: Geological Society of America Bulletin, V. 114, p. 1480–1504.

Rioux, M., Hacker, B., Mattinson, J., Kelemen, P., Blusztajn, J., and Gehrels, G., 2007, Magmatic development of an intra-oceanic arc: High-precision U-Pb zircon and whole-rock isotopic analyses from the accreted Talkeetna arc, south-central Alaska: Geological Society of America Bulletin, v. 119, p. 1168–1184, doi: 10.1130/B25964.1.

Roberge, J., Wallace, P.J., White, R.V., and Coffin, M.F., 2005, Anomalous uplift and subsidence of the Ontong Java Plateau inferred from CO_2 contents of submarine basaltic glasses: Geology, v. 33, p. 501–504, doi: 10.1130/G21142.1.

Roeske, S.M., Snee, L.W., and Pavlis, T.L., 2003, Dextral-slip reactivation of an arc-forearc boundary during Late Cretaceous–early Eocene oblique convergence in the northern Cordillera, *in* Sisson, V.B., et al., eds., Geology of a transpressional orogen developed during ridge-trench interaction along the North Pacific margin: Geological Society of America Special Paper 371, p. 141–169.

Sager, W.W., 2005, What built the Shatsky Rise, a mantle plume or ridge tectonics?, *in* Foulger, G.R., et al., eds., Plates, plumes, and paradigms: Geological Society of America Special Paper 388, p. 721–733.

Saleeby, J.B., 1983, Accretionary tectonics of the North American cordillera: Annual Review of Earth and Planetary Sciences, v. 11, p. 45–73, doi: 10.1146/annurev.ea.11.050183.000401.

Saltus, R.W., Hudson, T., and Wilson, F.H., 2007, The geophysical character of southern Alaska: Implications for crustal evolution, *in* Ridgway, K.D., et al., eds., Tectonic growth of a collisional continental margin: Crustal evolution of southern Alaska: Geological Society of America Special Paper 431, p. 1–20.

Samson, S.D., and Alexander, E.C., 1987, Calibration of the interlaboratory $^{40}Ar/^{39}Ar$ dating standard MMhb1: Chemical Geology, v. 66, p. 27–34.

Saunders, A.D., Jones, S.M., Morgan, L.A., Pierce, K.L., Widdowson, M., and Xu, Y.G., 2007, Regional uplift associated with continental large igneous provinces: The roles of mantle plumes and the lithosphere: Chemical Geology, v. 241, p. 282–318, doi: 10.1016/j.chemgeo.2007.01.017.

Schatz, W., 2005, Palaeoecology of the Triassic black shale bivalve Daonella—New insights into an old controversy: Palaeogeography, Palaeoclimatology, Palaeoecology, v. 216, p. 189–201, doi: 10.1016/j.palaeo.2004.11.002.

Schmidt, J.M., and Rogers, R.K., 2007, Metallogeny of the Nikolai large igneous province (LIP) in southern Alaska and its influence on the mineral potential of the Talkeetna Mountains, *in* Ridgway, K.D., et al., eds., Tectonic growth of a collisional continental margin: Crustal evolution of southern Alaska: Geological Society of America Special Paper 431, p. 623–648.

Schmidt, J.M., O'Neill, J.M., Snee, L.W., Blodgett, R.B., Ridgway, K.D., Wardlaw, B.R., and Blome, C.D., 2003a, The northwestern edge of Wrangellia: Stratigraphic and intrusive links between crustal block from the Peninsular terrane to Broad Pass: Geological Society of America Abstracts with Programs, v. 35, no. 6, p. 560.

Schmidt, J.M., Werdon, M.B., and Wardlaw, B., 2003b, New mapping near Iron Creek, Talkeetna Mountains, indicates presence of Nikolai greenstone, *in* Clautice, K.H., and Davis, P.K., eds., Short notes on Alaska geology 2003: Alaska Division of Geological and Geophysical Surveys Professional Report 120J, p. 101–108.

Schmidt, R., and Schmicke, H.U., 2000, Seamounts and island building, *in* Sigurdsson, H., ed., Encyclopedia of volcanoes: San Diego, California, Academic Press, p. 383–402.

Self, S., Thordarson, T., and Keszthely, L., 1997, Emplacement of continental flood basalt lava flows, *in* Mahoney, J.J. and Coffin, M.F., eds., Large igneous provinces: Continental, oceanic, and planetary flood volcanism: American Geophysical Union Geophysical Monograph 100, p. 381–410.

Sircombe, K.N., 2004, AGEDISPLAY: An EXCEL workbook to evaluate and display univariate geochronological data using binned frequency histograms and probability density distributions: Computers & Geosciences, v. 30, no. 1, p. 21–31, doi: 10.1016/j.cageo.2003.09.006.

Sluggett, C.L., 2003, Uranium-lead age and geochemical constraints on Paleozoic and early Mesozoic magmatism in Wrangellia Terrane, Saltspring Island, British Columbia [B.Sc. thesis]: Vancouver, University of British Columbia, 84 p.

Smith, J.G., and MacKevett, E.M., Jr., 1970, The Skolai Group in the McCarthy B-4, C-4, C-5 Quadrangles, Wrangell Mountains, Alaska: U.S. Geological Survey Bulletin 1274-Q, p. Q1–Q26.

Smith, P.L., 2006, Paleobiogeography and Early Jurassic molluscs in the context of terrane displacement in western Canada, *in* Haggart, J.W., et al., eds., Paleogeography of the North American Cordillera: Evidence for and against large-scale displacements: Geological Association of Canada Special Paper 46, p. 81–94.

Surdam, R.C., 1967, Low-grade metamorphism of the Karmutsen Group [Ph.D. dissertation]: Los Angeles, University of California, 288 p.

Taylor, B., 2006, The single largest oceanic plateau: Ontong Java-Manihiki-Hikurangi: Earth and Planetary Science Letters, v. 241, p. 372–380, doi: 10.1016/j.epsl.2005.11.049.

Thordarson, T., and Self, S., 1996, Sulfur, chlorine and fluorine degassing and atmospheric loading by the Roza eruption, Columbia River Basalt Group, Washington, USA: Journal of Volcanology and Geothermal Research, v. 74, p. 49–73, doi: 10.1016/S0377-0273(96)00054-6.

Trop, J.M., and Ridgway, K.D., 2007, Mesozoic and Cenozoic tectonic growth of southern Alaska: A sedimentary basin perspective, *in* Ridgway, K.D., et al., eds., Tectonic growth of a collisional continental margin: Crustal evolution of southern Alaska: Geological Society of America Special Paper 431, p. 55–94.

Trop, J.M., Ridgway, K.D., Manuszak, J.D., and Layer, P.W., 2002, Mesozoic sedimentary basin development on the allochthonous Wrangellia composite terrane, Wrangell Mountains basin, Alaska: A long-term record of terrane migration and arc construction: Geological Society of America Bulletin, v. 114, p. 693–717, doi: 10.1130/0016-7606(2002)114<0693:MSBDOT>2.0.CO;2.

Umhoefer, P.J., and Blakey, R.C., 2006, Moderate (1600 km) northward translation of Baja British Columbia from southern California: An attempt at reconciliation of paleomagnetism and geology, *in* Haggart, J.W., et al., eds., Paleogeography of the North American Cordillera: Evidence for and against large-scale displacements, Geological Association of Canada Special Paper 46, p. 307–329.

Wallace, P.J., 2002, Volatiles in submarine basaltic glasses from the Northern Kerguelen Plateau (ODP Site 1140): Implications for source region compositions, magmatic processes, and plateau subsidence: Journal of Petrology, v. 43, p. 1311–1326, doi: 10.1093/petrology/43.7.1311.

Wheeler, J.O., and McFeely, P., 1991, Tectonic assemblage map of the Canadian Cordillera and adjacent part of the United States of America: Geological Survey of Canada Map 1712A.

White, S.M., Crisp, J.A., and Spera, F.J., 2006, Long-term volumetric eruption rates and magma budgets: Geochemistry Geophysics Geosystems, v. 7, Q03010, doi: 10.1029/2005GC001002.

Wignall, P.B., 2001, Large igneous provinces and mass extinctions: Earth-Science Reviews, v. 53, p. 1–33, doi: 10.1016/S0012-8252(00)00037-4.

Wilson, F.H., Dover, J.D., Bradley, D.C., Weber, F.R., Bundtzen, T.K., and Haeussler, P.J., 1998, Geologic map of Central (Interior) Alaska: U.S. Geological Survey Open-File Report 98–133-A, http://wrgis.wr.usgs.gov/open-file/of98-133-a/.

Wilson, F.H., Labay, K.A., Shew, N.B., Preller, C.C., Mohadjer, S., and Richter, D.H., 2005, Digital data for the geology of Wrangell-Saint Elias National Park and Preserve, Alaska: U.S. Geological Survey Open-File Report 2005–1342, http://pubs.usgs.gov/of/2005/1342/.

Yole, R.W., 1969, Upper Paleozoic stratigraphy of Vancouver Island, British Columbia: Geological Association of Canada Proceedings, v. 20, p. 30–40.

Yorath, C.J., Sutherland Brown, A., and Massey, N.W.D., 1999, LITHOPROBE, southern Vancouver Island, British Columbia: Geological Survey of Canada Bulletin 498, 145 p.

Manuscript Received 9 October 2008
Revised Manuscript Received 29 June 2009
Manuscript Accepted 9 August 2009

Erratum

The architecture of oceanic plateaus revealed by the volcanic stratigraphy of the accreted Wrangellia oceanic plateau
Andrew R. Greene, James S. Scoates, Dominique Weis, Erik C. Katvala, Steve Israel, and Graham T. Nixon
(v. 6, no. 1, p. 47–73; doi: 10.1130/GES00212.1)
Figure 8 appeared incorrectly. The corrected figure follows: